

# 1        **Tectonic setting and isotopic sources (Sm-Nd) of the SW**

## 2                    **Iberian Autochthon (Variscan Orogen)**

3  
4  
5 José M. Fuenlabrada<sup>1\*</sup>, Ricardo Arenas<sup>2</sup>, Rubén Díez Fernández<sup>3</sup>, José González del  
6 Tánago<sup>2</sup>, Luis Miguel Martín-Parra<sup>3</sup>, Jerónimo Matas<sup>3</sup>, Esther Rojo-Pérez<sup>2</sup>, Sonia  
7 Sánchez Martínez<sup>2</sup>, Pilar Andonaegui<sup>2</sup>, Byron Solis Alulima<sup>2</sup>

8  
9 1 Unidad de Geocronología (CAI de Ciencias de la Tierra y Arqueometría). Universidad Complutense,  
10 Madrid, Spain.

11 2 Departamento de Mineralogía y Petrología e Instituto de Geociencias (UCM, CSIC), Universidad  
12 Complutense, Madrid, Spain.

13 3 Instituto Geológico y Minero de España, 28760 Tres Cantos, Madrid, Spain.

14  
15  
16 \* *Corresponding author at Unidad de Geocronología (CAI de Ciencias de la Tierra y*  
17 *Arqueometría), Universidad Complutense de Madrid. Facultad de Ciencias Geológicas.*  
18 *Calle José Antonio Novais 12. 28040 Madrid. Spain.*

19  
20 *E-mail address: [jmfuenla@ucm.es](mailto:jmfuenla@ucm.es) (José Manuel Fuenlabrada, corresponding author)*

21  
22 E-mail addresses:

23 [jmfuenla@ucm.es](mailto:jmfuenla@ucm.es) (José M. Fuenlabrada)

24 [rarenas@ucm.es](mailto:rarenas@ucm.es) (Ricardo Arenas)

25 [r.diez@igme.es](mailto:r.diez@igme.es) (Rubén Díez Fernández)

26 tanago@geo.ucm.es (José González del Tánago)

27 lm.martin@igme.es (Luis Miguel Martín-Parra)

28 j.matas@telefonica.net (Jerónimo Matas)

29 e.rojo@ucm.es (Esther Rojo-Pérez)

30 s.sanchez@geo.ucm.es (Sonia Sánchez Martínez)

31 andonaeg@geo.ucm.es (Pilar Andonaegui)

32 bysolis@ucm.es (Byron Solis Alulima)

33

34

35 **Abstract**

36

37 Metasedimentary rock successions in Sierra Albarrana Group (SW Iberia Autochthonous  
38 Domain) were deposited during the Early Paleozoic influenced by the evolution of a peri-  
39 Gondwanan active margin. Their geochemical composition indicates dominant  
40 contributions from felsic igneous sources and an upper continental crust provenance. The  
41 high mineralogical and geochemical maturity, together with negative  $\epsilon\text{Nd}_{(530)}$ , ranging  
42 from -11.3 to -4.5, and old Nd model ages (TDM: 1388-1897 Ma) imply reworked  
43 materials from old continental source areas with a limited juvenile contribution for the  
44 siliciclastic sedimentary rocks in Sierra Albarrana. Both, geochemical and isotope  
45 features were caused by the progressive denudation of rocks bearing the isotopic imprint  
46 from an old basement exposed along the Gondwanan margin. The paleobasin for the SW  
47 Iberia Autochthon probably occupied an outboard position across the peri-Gondwanan  
48 margin during Ediacaran-Cambrian times. In a convergent scenario, the interaction  
49 between the peri-Gondwanan trench and the external part of the continent generated  
50 tectonic uplift, giving way to exposure of crust formed during earlier stages of the

51 Cadomian Orogeny and erosion. Sediment redistribution through Early Paleozoic times  
52 supplied recycled detrital materials, which likely filled a retro-arc basin formed after the  
53 switch from an extensional to a compressional regime in the upper plate of the Cadomian  
54 Orogen that is recorded throughout the peri-Gondwanan domain of Iberia. A subsequent  
55 extensional stage led to a progressive widening of its marginal basins, thus bringing the  
56 onset of a passive margin from the Cambro-Ordovician onwards. Nd model ages of the  
57 Sierra Albarrana Group overlap those of Early Cambrian series from the southernmost  
58 Central Iberian Zone, and are considered an indication for the paleogeographic closeness  
59 between all these sequences during Cambrian times, occupying eastern positions closer  
60 to Tuareg Shield and the Sahara Metacraton sections along the Gondwanan margin.

61

62 Keywords: Iberian Massif, Sm-Nd isotope geochemistry, SW autochthonous domain,  
63 Sierra Albarrana Group, Gondwanan paleogeography.

64

## 65 **Resumen**

66

67 Las series de rocas metasedimentarias en el Grupo Sierra Albarrana (Dominio Autóctono  
68 del SW de Iberia) se depositaron durante el Paleozoico Inferior, influidas por la evolución  
69 de un margen activo peri-Gondwánico. Su composición geoquímica indica una  
70 contribución dominante desde fuentes ígneas félsicas con afinidad con una corteza  
71 continental superior. La elevada madurez mineralógica y geoquímica, junto con valores  
72 negativos de  $\epsilon\text{Nd}_{(530)}$  (-11.3 a -4.5) y edades modelo de Nd relativamente antiguas (TDM:  
73 1388-1897 Ma), implica materiales retrabajados desde áreas fuente continentales  
74 antiguas, con una contribución juvenil limitada para las rocas siliciclásticas estudiadas en  
75 el Grupo Sierra Albarrana. Sus características geoquímicas e isotópicas fueron fruto de

76 una denudación progresiva de rocas con una composición isotópica afín a un basamento  
77 antiguo expuesto a lo largo del margen de Gondwana. Teniendo en cuenta la información  
78 disponible para el SW del Macizo Ibérico, la paleocuenca del Dominio Autóctono del SW  
79 de Iberia probablemente ocupó posiciones externas en el margen peri-Gondwánico  
80 durante la transición Ediacárico-Cámbrico. En un contexto de convergencia, la  
81 interacción entre la trinchera peri-Gondwánica y la parte externa del continente ocasionó  
82 probablemente un levantamiento tectónico pronunciado, dando lugar a la exposición y  
83 posterior erosión de la corteza continental peri-Gondwánica formada durante las etapas  
84 iniciales de la Orogenia Cadomiense. La redistribución de sedimentos durante el  
85 Paleozoico Inferior aportó materiales detríticos reciclados, que probablemente rellenaron  
86 una cuenca retro-arco, formada tras el cambio de un régimen compresivo a uno  
87 extensional en la placa superior del Orógeno Cadomiense y que se registra a lo largo de  
88 todo el dominio peri-Gondwánico de Iberia. El avance en la extensión condujo a un  
89 progresivo ensanchamiento de las cuencas marginales, marcando el inicio de un margen  
90 pasivo desde el periodo Cambro-Ordovícico en adelante. Las edades modelo de Nd del  
91 Grupo Sierra Albarrana se solapan con las obtenidas en series del Cámbrico Inferior del  
92 sur de la Zona Centro Ibérica, y se consideran indicadoras de una cercanía  
93 paleogeográfica entre estas secuencias durante el Cámbrico, ocupando posiciones  
94 relativamente orientales, cercanas al Escudo de Tuareg y al Metacratón del Sahara.

95

96 **Palabras clave:** Macizo Ibérico, Geoquímica isotópica Sm-Nd, Dominio Autóctono del  
97 SW, Grupo Sierra Albarrana, Paleogeografía de Gondwana

98

99 **1. Introduction**

100

101 In the latest years, many works have focused on understanding the magmatic and tectonic  
102 events that took place during the Neoproterozoic and Early Paleozoic in the peri-  
103 Gondwanan magmatic arc-systems related to the Cadomian Orogeny (e.g., Murphy and  
104 Nance, 1989; Ballèvre et al., 2001; Linnemann and Romer, 2002; von Raumer et al.,  
105 2002; Pereira et al., 2006; Linnemann et al., 2014; Andonaegui et al., 2016; Arenas et al.,  
106 2018; Díez Fernández et al., 2019). This effort has gone hand by hand with an aim to  
107 deciphering the relative position of Variscan terranes along the paleomargin of Gondwana  
108 before its Devonian collision against Laurussia, figuring out in the way the  
109 paleogeography of the Ediacaran paleomargin of Gondwana (e.g., Díez Fernández et al.,  
110 2010; Ábalos et al., 2012; Avigad et al., 2012; Pereira et al., 2012a, 2020; Fernández  
111 Suárez et al., 2014; Stephan et al., 2019a, 2019b; Fuenlabrada et al., 2020). Geochemical,  
112 isotopic and geochronological approaches have become highly important to identify the  
113 provenance of the Iberian terranes. U-Pb-Hf geochronology and isotope geochemistry in  
114 detrital zircons have grown into a useful mean in providing paleogeographic models for  
115 their Gondwanan provenance (e.g., Fernández-Suárez et al., 2000, 2003, 2014; Ugidos et  
116 al., 2003a; Pereira et al., 2008, 2012a; Bea et al., 2010; Díez Fernández et al., 2010;  
117 Ábalos et al., 2012; Talavera et al., 2012; Albert et al., 2015; Orejana et al., 2015;  
118 Herderson et al., 2016) and for constraining the tectonothermal history and the particular  
119 provenance of correlative European terranes (e.g., Linnemann et al., 2007; Drost et al.,  
120 2011; Avigad et al., 2012, 2018; Abbo et al., 2015; Arenas et al., 2016a; Collet et al.,  
121 2020; Martínez Catalán et al., 2020).

122

123 Together with the development of U-Pb-Hf geochronological and isotope geochemistry  
124 tools, whole-rock geochemistry and Nd-isotope composition studies in metasedimentary  
125 rock sequences have provided new data to improve the understanding about the

126 provenance and the probable depositional environment of the Iberian metasedimentary  
127 record (e.g., Nägler et al., 1995; Ugidos et al., 2003b; López-Guijarro et al., 2008; Bea et  
128 al., 2010; Fuenlabrada et al., 2010, 2012, 2016; Pastor-Galán et al., 2013; Fernández-  
129 Suárez et al., 2014; Villaseca et al., 2014; Díez Fernández et al., 2017; Rojo-Pérez et al.,  
130 2019). An extensive sedimentary record in the Iberian Massif has allowed the study of  
131 the late Ediacaran evolution of a peri-Gondwanan active margin and its subsequent  
132 transition to a passive margin during Cambrian-Ordovician times (Rodríguez-Alonso et  
133 al., 2004b; Pereira et al., 2006; Linnemann et al., 2008; Sánchez-García et al., 2008, 2014;  
134 Fuenlabrada et al., 2020). Geochemical and Nd-isotope data from Iberian terranes have  
135 provided evidence for changes in the depositional settings by that time. The filling of a  
136 peri-Gondwanan back-arc basin, strongly influenced by ongoing magmatic activity,  
137 occurred during Ediacaran times (Fuenlabrada et al., 2012, 2016; Pereira et al., 2012a;  
138 Fernández-Suárez et al., 2014). The subsequent widening of that basin during the Early  
139 Cambrian period led to a change in the siliciclastic contributions to more recycled and  
140 older detritus (Fuenlabrada et al., 2020). The Nd-isotope information from siliciclastic  
141 series of the Iberian Massif represents an effective and comparative method for  
142 paleoreconstructions of the current Iberian terranes during the Neoproterozoic and  
143 Paleozoic times (Fernández-Suárez et al., 2014; Albert et al., 2015; Cambeses et al., 2017;  
144 Fuenlabrada et al., 2020), allowing a comparison between tectonostratigraphic units,  
145 members of the same terrane, but currently dispersed over the Iberian Massif due to  
146 superimposed deformation.

147

148 The current disposition of domains in the Iberian Massif was the result of the Pangea  
149 assembly during the Devonian through to the Carboniferous period after the closure of  
150 the Rheic and other oceanic basins (Franke, 1989; Matte, 1991; Winchester et al., 2002;

151 von Raumer et al., 2003; Nance et al., 2010; Stampfli et al., 2013). The collision between  
152 Gondwana and Laurussia raised the Variscan Orogen (Fig. 1a), which is featured by  
153 suture zones and far-traveled (allochthonous) terranes that spread over the Iberian Massif  
154 and onto autochthonous sections of the margin of Gondwana (Fig. 1b) (Martínez Catalán  
155 et al., 1997, 2007; Ribeiro et al., 2007; Simancas et al., 2009; Arenas et al., 2014, 2016a;  
156 Díez Fernández and Arenas, 2015; Díez Fernández et al., 2016). The generally accepted  
157 criterion for defining the autochthonous character of Iberian terranes has been their lower  
158 (plate) structural position relative to Variscan suture zone exposures (e.g., Ries and  
159 Shackleton, 1971; Arenas et al., 1986, 2016a; Simancas et al., 2003; Martínez Catalán et  
160 al., 2020 and references therein). This is many times accompanied by a particular  
161 metamorphic evolution during the Variscan accretionary history, which makes them  
162 different from the Iberian allochthonous sections, i.e. a Barrovian-type evolution and a  
163 usual lack of high-P metamorphism (Dallmeyer et al., 1997; Martínez Catalán et al., 2009;  
164 Díez Fernández et al., 2016). The autochthonous sections represent inboard domains of  
165 the North African margin of Gondwana and include pre-Variscan metasedimentary  
166 sequences that range between Ediacaran and Devonian in age (Alvarez Nava et al., 1988;  
167 Gutierrez-Marco et al., 1990; San José et al., 1990; Valladares et al., 2000, 2002;  
168 Rodríguez Alonso et al., 2004a).

169

170 Here we present a new comprehensive whole-rock and Nd-isotope geochemical data set  
171 from the metasedimentary rocks cropping out in an autochthonous section of the SW  
172 Iberian Massif, locally referenced to as the Sierra Albarrana Group. Major and trace  
173 elements showing low-mobility characteristics during weathering, sedimentary transport,  
174 and post-depositional processes, would provide clues to track the influence of the  
175 geodynamic frame over the development and evolution of the sedimentary basins in

176 which the sedimentary protoliths of the Sierra Albarrana Group were deposited.  
177 Similarly, this geochemical and isotope approach would contribute to constrain the  
178 provenance and relative paleoposition of this autochthonous section of the Variscan  
179 Orogen relative to other peri-Gondwanan terranes of the Iberian Massif, with particular  
180 focus on other autochthonous sequences of the Iberian Variscides that are now exposed  
181 in the southernmost section of the Central Iberian Zone (Fuenlabrada et al., 2016), i.e. the  
182 closest ones to the study case.

183

## 184 **2. Geological setting**

185

186         The first division of the Iberian Massif made by Lotze (1945) and Julivert et al.  
187 (1972) resulted in several geotectonic zones (Cantabrian, West Asturian-Leonese, Central  
188 Iberian, Ossa-Morena, and South-Portuguese zones). They show particular stratigraphic,  
189 structural, magmatic and metamorphic features, defining external or more internal  
190 domains within the southernmost section of the Variscan Orogen (Fig. 1a) (Martínez  
191 Catalán et al., 2009; Simancas et al., 2009; Arenas et al., 2014; Díez Fernández et al.,  
192 2016). After that initial division, several authors have contributed with new data and  
193 perspectives towards a further discrimination of geotectonic zones (e.g. Galicia-Trás-os-  
194 Montes Zone; Farias et al., 1987). Certain domains that constitute these geotectonic zones  
195 preserve particular characteristics from the earlier Variscan orogenic imprint, tightly  
196 connected to continental subduction (Fernández-Suárez et al., 2002a; Stampfli et al.,  
197 2002; Martínez Catalán et al., 2009; Kroner and Romer, 2013; Rubio Pascual et al., 2013;  
198 Albert et al., 2015; Arenas et al., 2016a). Devonian high-P metamorphism and/or peri-  
199 Gondwanan paleoposition are typical features for the terranes that are thrust onto inboard  
200 sections of Gondwana in Iberia, the latter being the autochthon to a suture zone and its



201 upper plate that can now be observed as allochthonous dismembered pieces over the  
202 Iberian Massif (Díez Fernández and Arenas, 2015). This allochthonous – autochthonous  
203 pair is the essence to the distinction of allochthonous complexes in NW Iberia, and can  
204 be also observed in the SW of the Iberian Massif. As a result, most of the former Ossa-  
205 Morena Zone emerged as a new allochthonous complex, composed by terranes with  
206 different origin and tectonothermal evolution, while the sections underlying this complex  
207 became part of the Iberian Autochthon (Fig. 1b; Díez Fernández and Arenas, 2015).

208

209 The Ossa-Morena Complex preserves typical features for a North Gondwanan margin  
210 provenance (López-Guijarro et al., 2008; Pereira et al., 2008, 2012b; Rojo-Pérez et al.,  
211 2019), with a pre-Variscan (Ediacaran to Devonian) metasedimentary and metaigneous  
212 record (Fig. 2). The Cadomian tectonothermal history is linked to the geodynamic activity  
213 of a peri-Gondwanan continental arc during Ediacaran and Cambrian times (Eguíluz et  
214 al., 2000; Pereira et al., 2006; Linnemann et al., 2008; Díez Fernández et al., 2017, 2019;  
215 Arenas et al., 2018; Rojo-Pérez et al., 2019). In that context, the Ediacaran  
216 metasedimentary rocks constituting the so-called Serie Negra Group (Carvalhosa, 1965)  
217 define the basal part of an upper allochthonous terrane (Díez Fernández and Arenas, 2015;  
218 Arenas et al., 2016b; Díez Fernández et al., 2016), and although it appears widely  
219 throughout the complex, it is especially important in the central area of the Olivenza-  
220 Monesterio antiform (Eguíluz, 1987; Quesada et al., 1990) (Fig. 2). The Serie Negra  
221 Group has been traditionally divided into the Montemolín and Tentudía formations  
222 (Eguíluz, 1987). Occupying the lower part of the series, the Montemolín Formation is  
223 mainly composed by metasandstones (including black quartzites), mica-schists, and  
224 abundant intercalations of metabasites. The maximum depositional age for this formation  
225 has been estimated at  $591 \pm 11$  Ma (U-Pb in detrital zircons; Ordoñez Casado et al., 2009).

226 The protoliths of this formation have been interpreted as related to a passive margin  
227 setting (Quesada, 1990; Cambeses et al., 2017), although their geochemical composition  
228 suggests the influence of a Cadomian volcanic arc during their sedimentation (López  
229 Guijarro, 2006; Rojo-Pérez et al., submitted). The Tentudía Formation, as well as the Don  
230 Alvaro and Oliva de Mérida Successions (Bandrés et al., 2001), rest on top and includes  
231 metagreywackes, black metapelites, black quartzites and felsic metaigneous rocks and  
232 minor metabasites. The study of U-Pb in detrital zircons from the sedimentary protoliths  
233 of this formation yielded a maximum depositional age of 560-544 Ma (Schäfer et al.,  
234 1993; Ordóñez-Casado et al., 1998; Fernández Suárez et al., 2002b; Linnemann et al.,  
235 2008), with a probable deposition linked to the evolution of a back-arc basin (Bandrés,  
236 2001; Cambeses et al., 2017; Rojo-Pérez et al., 2019, submitted). Overlying discordantly,  
237 the volcanoclastic Malcocinado Formation (Fricke, 1941), with igneous intrusions (El  
238 Escribano, El Mosquil, La Bomba; Sánchez Carretero et al., 1989), probably contains the  
239 boundary between Ediacaran and Cambrian times (Pereira, 2015a), while the discordant  
240 sequences of the Torreárboles Formation, mainly composed by metasandstones and  
241 metaconglomerates, have been attributed to the Early Cambrian (Liñan and Palacios,  
242 1983; Liñan, 1984; Liñan et al., 1984). The Central, Cubito-Moura, and Escoural units  
243 (Fig. 1b) are members of a terrane that is located at the base of the allochthonous nappe  
244 pile (Basal Allochthonous Units), i.e. underlying the upper allochthonous terrane cited  
245 above (Uppermost Allochthonous Units) and on top of the Autochthon to the Ossa-  
246 Morena Complex (Fig. 1b). The three of them, especially the Central Unit, have  
247 continental crust affinity, peri-Gondwanan provenance (Díez Fernández et al., 2017) and  
248 experienced Devonian high-P metamorphism (Moita et al., 2005; Abati et al., 2018).  
249

250 The Sierra Albarrana Group (Delgado Quesada, 1971; Garrote, 1976; Azor, 1994;  
251 González del Tánago, 1995) is exposed immediately to the SW of the Badajoz-Córdoba  
252 Shear Zone, classically considered as the boundary between the Ossa-Morena Zone and  
253 the southernmost section of the Central Iberian Zone (Robardet, 1976; Martínez Poyatos,  
254 1997; Pérez Estaún et al., 2004) (Fig. 2), where a dip-slip Variscan extensional fault is  
255 presented (Martín Parra et al., 2006). The best exposures of the Sierra Albarrana Group  
256 are located to the south of the Azuaga Fault (Chacón et al., 1974; Delgado Quesada et al.,  
257 1977; Apalategui et al., 1985; Ábalos et al., 1990), and resting under the Central Unit as  
258 an autochthonous section of the Variscan Orogen (Azor, 1994; and references therein).  
259 According to González del Tánago and Peinado (1990), the tectonometamorphic  
260 evolution of this group defines it as a NW-SE elongated thermal dome, dominated by  
261 metasedimentary rocks and minor metabasites, folded into an antiformal structure. The  
262 Sierra Albarrana Group is composed mainly of four different lithostratigraphic  
263 successions, with a dominant siliciclastic character, from bottom to top: (i) Albarrana  
264 Succession (AS), (ii) Cabril-Peña Grajera Succession (CGS), (iii) Albariza-Bembézar  
265 Succession (ABS), and (iv) Azuaga Formation (AzF) (Fig. 3).  
266  
267 González del Tánago y Peinado (1990) included the first two aforementioned units into a  
268 single one (Albarrana Gneisses Unit) that occupies the core of the antiformal structure,  
269 and consisting of rocks fairly different from the dominant schistose or phyllitic nature of  
270 the rocks in the rest of the units. The Albarrana Succession (also named as Albarrana  
271 Quartzites or Albarrana Formation by Delgado Quesada, 1971 and Garrote et al., 1980,  
272 respectively) occupies the central area of the dome structure and it is mainly composed  
273 of quartzites (mainly feldspathic), paragneisses, with minor schists, migmatites,  
274 pegmatitic bodies and lenses of amphibolite. The paragneisses are essentially meta-

275 arkoses with a predominant monotonous quartz-feldspathic composition (González del  
276 Tánago, 1995). The Cabril-Peña Grajera Succession rests on top of the Albarrana  
277 Succession and consists mainly of paragneisses, migmatites, fine-medium grain sized  
278 metasediments, feldspathic quartzites and minor schists, most of which derive from  
279 semipelitic and pelitic protoliths. This unit corresponds to the Blastomylonitic Formation  
280 and Cabril-Peña Grajera Formation defined by Delgado Quesada (1971) and Garrote et  
281 al. (1980), respectively, and Insúa et al. (1991) distinguished an additional member made  
282 of paragneisses and schists referred to as the Cerro Pavillos Succession (Fig. 3). The  
283 gneisses and migmatites of this unit are characterized by penetrative tectonic banding  
284 defined by quartz-feldspathic and biotite-rich layers (Azor, 1994). The metasedimentary  
285 rocks so far described preserve primary sedimentary structures such as ripples and cross-  
286 bedding, and were considered as intertidal deposits with an important contribution from  
287 felsic volcanic sources by González del Tánago (1995; and references therein).

288

289 The Albariza-Bembézar Succession (Albariza-Bembézar Schist Unit; González del  
290 Tánago, 1995) rests on top of the Cabril-Peña Grajera Succession (Fig. 3). Despite being  
291 divided into two formations according to their position in the NE or SW limb of the  
292 antiformal structure of the region (La Albariza and Bembézar formations; Delgado  
293 Quesada, 1971; Garrote et al., 1980), their lithostratigraphic similarity, lateral structural  
294 continuity and metamorphic homogeneity were taken as solid grounds to merge them into  
295 a single succession, which may show some local minor differences regarding the  
296 abundance in amphibolite layers, pegmatites, or in the size of staurolite and garnet  
297 porphyroblasts (Insúa et al., 1991; González del Tánago, 1995). This unit is mainly  
298 composed by a metapelitic succession of schists, amphibolite lenses, garnet-bearing  
299 amphibolites (González del Tánago and Arenas, 1991), interbedded with minor

300 metasediments and white quartzites, and dykes of diabase. Pegmatitic bodies can be  
301 found close to the contact with the Albarrana Succession, where it shows higher strain  
302 and incipient migmatization.

303

304 The Azuaga Formation mantles the antiform structure of the study area and occupies the  
305 upper structural position within the Sierra Albarrana Group (Fig. 3). The Azuaga  
306 Formation is separated from the so-called Central Unit (Azor et al., 1994) (Fig. 1b) by the  
307 Azuaga Fault, and from the rest of the Ossa-Morena Complex to the SW by the Onza and  
308 Malcocinado faults (Azor, 1994). However, materials that can be correlated with those  
309 found in the Albariza-Bembézar Succession, and mainly in Azuaga Formation are found  
310 in a thrust sheet located to the north of the Central Unit (Fig. 2). The current juxtaposition  
311 of this unit onto the rest of the Sierra Albarrana Group was interpreted to have been  
312 carried out by the Casa del Café Fault (Azor, 1994). The Azuaga Formation shows low-  
313 grade metamorphism, and consists of fine-grained metasedimentary sequences with  
314 turbiditic origin, mainly composed of characteristic laminated slates, as well as phyllites,  
315 minor quartzite intercalations, post-metamorphic dykes of diabase and some mica-schists  
316 towards the lower part of the series (González del Tánago, 1995). The Cardenchoa pluton  
317 intruded this unit and produced contact metamorphism in its host (Insúa et al., 1991). This  
318 pluton is affected by Variscan deformation (Simancas et al., 2000), has been dated at  
319 Early Ordovician and interpreted as part of a late-rift episode, related to the Cambrian-  
320 Ordovician rift stage of the Iberian Massif (Azor et al., 2016; Sánchez García et al., 2019).

321

322 The successions here described were affected by several phases of deformation  
323 (Dallmeyer and Quesada, 1992; Azor et al., 2004, 2012). Earlier deformation was  
324 accompanied by intermediate-P metamorphism, which evolved to lower-P conditions in

325 the whole set and to higher-T conditions towards the lower structural section (González  
326 del Tánago and Peinado, 1990). This gave rise to a normal metamorphic zonation from  
327 the biotite zone on top up to partial melting conditions towards the bottom (Garrote, 1976;  
328 González del Tánago, 1995). The penetrative metamorphic fabrics formed in this area  
329 were considered as formed in relation to a ductile shear zone (Azor and Ballèvre, 1997),  
330 while the upright folds that affect the series were interpreted as Variscan and related to  
331 strike-slip shear zones (Simancas et al., 2000).

332

333 The age of the successions in Sierra Albarrana has been traditionally attributed to  
334 Precambrian times (Delgado Quesada 1971, Garrote, 1976, Garrote et al., 1980, Quesada  
335 et al., 1990; López-Guijarro et al., 2008), although a correlation between the quartzites in  
336 the Albarrana Succession and the Ordovician Armorican Quartzite of the Central Iberian  
337 Zone was made by Apalategui et al. (1985). In the quartzites of the Albarrana Succession,  
338 ichnofossils, such as *Monocraterion*, suggest sedimentation in a shallow marine  
339 environment from Early Cambrian times onward (Azor et al., 1991; Marcos et al., 1991).  
340 López-Guijarro et al. (2008) ruled out a deposition age younger than Ordovician for the  
341 sedimentary series in Sierra Albarrana according to the deformation, metamorphism and  
342 intrusion of granitoids in Early Ordovician times, thus being a record prior to the  
343 Ordovician rifting of the Iberian Massif. The fossil content in the Azuaga Formation has  
344 provided an Early-Middle Cambrian age to this series (Azor, 1994; Liñán, 1978; Liñán  
345 and Quesada, 1990; Jensen et al., 2004). Therefore, an Early Cambrian age can be  
346 attributed to the units of the Sierra Albarrana Group from the Azuaga Formation  
347 downwards (Azor, 1994; Azor and Ballèvre, 1997; Jensen et al., 2004).

348

349 **3. Whole rock geochemistry**

350

351 *3.1. Rock sampling and petrography*

352

353 Thirty one samples of siliciclastic rocks (3 feldspathic quartzites and 28 meta-  
354 sandstones/meta-shales) were collected from the four successions of the Sierra Albarrana  
355 Group (Fig. 3). Table 1 shows sample details, including their location, while Figure 4  
356 illustrates their main petrographic features. The three quartz-feldspathic samples of the  
357 Albarrana Succession (ALBA-01 to ALBA-03) are essentially composed of Qz and Pl,  
358 with Ms, Bt, and Kfs, and Rt as main accessory (mineral abbreviations after Whitney and  
359 Evans, 2010) (Fig. 4a). Among the meta-sandstones and meta-shales, eight samples were  
360 collected from the Cabril-Peña Grajera Succession (ALBA-04 to ALBA-11). They are  
361 fine-grained, grey-greenish, low strained rocks that change to medium-grained textures  
362 near quartzite layers (ALBA-09 to ALBA-11). The mineral assemblage observed in these  
363 rocks is composed of Qz, Pl, Kfs, Bt, Ms and Sil, with Tur and opaque as main accessory  
364 minerals (Fig. 4b and c). Fourteen metasedimentary rocks were collected in the Albariza-  
365 Bembézar Succession (ALBA-12 to ALBA-25). They consist of fine to medium-grained  
366 phyllites, mica-schists, and metagreywackes which may contain Grt, St, And, Sil, Qz, Pl,  
367 Bt, Ms, Chl, with Tur and opaque as the main accessory minerals. They define a  
368 metamorphic sequence with rapid decreasing P-T conditions from bottom to top (Fig. 4d,  
369 e, and f). Finally, six fine-grained phyllites and metagreywackes were collected in the  
370 Azuaga Formation (ALBA-26 to ALBA-31). They present a lepidoblastic fabric with Qz,  
371 Pl, Bt, Ms, and Chl as the most frequently observed minerals (Fig. 4g and h).

372

373 *3.2. Analytical methods*

374

375 Geochemical and isotope analyses were performed on firstly crushed and powdered rock  
376 samples at Universidad Complutense de Madrid (Spain). Major and trace elements were  
377 analyzed at Activation Laboratories Ltd. (Actlabs – Canada) following a fusion sample  
378 digestion with lithium metaborate or tetraborate, and ICP-OES (for major elements and  
379 Sc, Be, V, Zr, Ba, and Sr) and ICP-MS (for the rest of trace elements) analytical  
380 procedures. Along with the samples, two sample duplicates, two procedural method  
381 blanks, and fourteen international standards materials were analyzed in order to verify the  
382 quality of the analyses. The complete list of these certified and measured results are  
383 included in Supplementary Quality Control Table. The detection limits for the analytical  
384 procedure range from 0.01% for the majority of the major elements to 0.001% for TiO<sub>2</sub>  
385 and MnO; and for the trace elements, from 0.002 ppm for the Lu to 30 ppm for the Zn  
386 contents. Resulting data for the major and trace elements geochemical analysis are given  
387 in Table 2, and in Table 3 for Rare Earth Elements (REE).

388

389 Sm-Nd isotope analyses (Table 4) were performed at Geochronological Service of  
390 Universidad Complutense de Madrid, using Isotope Dilution Mass Spectrometry (ID-  
391 TIMS). Samples were spiked with a mixed <sup>149</sup>Sm-<sup>150</sup>Nd tracer before performing a sample  
392 dissolution with ultraclean reagents (HF-HNO<sub>3</sub>-HCl). The resulting solutions were  
393 passed through a double step chromatographic separation, by using DOWEX AG<sup>®</sup>50x8,  
394 in order to separate the complete REE group from the bulk matrix of the sample and in a  
395 second stage, LnResin<sup>®</sup> (Eichrom Technologies, Inc., USA) for a complete separation of  
396 Sm and Nd. Both purified fractions were loaded, together with 1 µl of ultrapure 0.05M  
397 H<sub>3</sub>PO<sub>4</sub>, on a pre-cleaned Re triple-filament arrangement and analyzed on an IsotopX-  
398 Phoenix<sup>®</sup> mass spectrometer (TIMS), following a single and a multi-dynamic collection  
399 procedure for Sm and Nd analysis, respectively. A normalized value of 0.7219 for the



400  $^{146}\text{Nd}/^{144}\text{Nd}$  ratio (O’Nions et al., 1979) was considered for a continuous correction of the  
401 Nd-isotope fractionation. Likewise, corrections for the presence of  $^{142}\text{Ce}$  and  $^{144}\text{Sm}$   
402 isotopes were continuously performed to prevent isobaric interferences during the  
403 analysis. Seven replicas of the Nd-reference standard JNdi-1 (Tanaka et al., 2000) were  
404 run along with the samples, yielding an average value of  $^{143}\text{Nd}/^{144}\text{Nd} = 0.512107$ , with  
405 an internal precision of  $\pm 0.000005$  ( $2\sigma$ ). Analytical errors on  $^{147}\text{Sm}/^{144}\text{Nd}$  and  
406  $^{143}\text{Nd}/^{144}\text{Nd}$  ratios were estimated at less than 0.1% and 0.006%, respectively, with a total  
407 Sm and Nd procedural method blank under 0.1 ng.

408

### 409 *3.3. Results*

410

#### 411 *3.3.1. Geochemical classification*

412

413 Major and trace elemental concentrations are given in Table 2. When plotting the major  
414 elements on the Herron (1988) geochemical classification diagram (Fig. 5a), the majority  
415 of the fine and medium-grained schistose samples plot in the shale field, closer to the Post  
416 Archean Australian Shale (PAAS; Taylor and MacLennan, 1985), some of them closer to  
417 the limit with the wacke field, matching stronger sandy features observed in the  
418 petrographic study (Table 1), and higher  $\text{SiO}_2/\text{Al}_2\text{O}_3$  ratios (Table 2). Five samples fall  
419 within the wacke field (ALBA-04, -06, -07, -23, and -31), which confirms field and  
420 petrographic observations. Meanwhile, quartzites samples from the Albarrana Succession  
421 (AS) plot in the arkose field, displaying the lowest values for the  $\text{SiO}_2/\text{Al}_2\text{O}_3$  ratios and  
422 very low K-contents (Fig. 5b). From the arkosic and relative immature character of the  
423 Albarrana quartzites, an increase of the sedimentary maturity can be observed from the  
424 Cabril-Peña Grajera Succession (CGS) to the Albariza-Bembézar Succession (ABS) and

425 Azuaga Formation (AzF) samples. Samples from these two latter successions share a  
426 similar geochemical composition. AS and CGS samples show higher  $\text{SiO}_2/\text{Al}_2\text{O}_3$  (8.30  
427 and 4.17, respectively) and lower  $\text{K}_2\text{O}/\text{Na}_2\text{O}$  ratios (0.12 and 1.86, respectively) than  
428 those observed in the PAAS (3.32 and 3.08, respectively). The latter implies a relative  
429 immature character, with a predominance of plagioclase over K-feldspar, compatible with  
430 very low values of  $\text{K}_2\text{O}$  in the quartzite samples (avg. 0.37 wt.%) (Fig. 5b). High  $\text{SiO}_2$   
431 contents (82.25 wt.% and 63.75 wt.%, avg. values for AS and CGS, respectively) and  
432 particularly a relative lower  $\text{Al}_2\text{O}_3$  abundances (10.14 wt.% and 15.81 wt.%, avg. values  
433 for AS and CGS, respectively) are probably related to a limited presence of micas, as  
434 confirmed by a negative or very poor correlation between Al, Fe, and K in the samples  
435 from these two units. On the contrary, the metasedimentary samples from the ABS and  
436 AzF show lower  $\text{SiO}_2$  and higher  $\text{Al}_2\text{O}_3$  abundances (60.10 and 63.91 wt.%, and 20.60  
437 and 18.18 wt.%, respectively), with  $\text{SiO}_2/\text{Al}_2\text{O}_3$  (3.10 and 3.57) and  $\text{K}_2\text{O}/\text{Na}_2\text{O}$  ratios  
438 (2.85 and 2.24) closer to those of the PAAS, indicating a strong pelitic character, in  
439 agreement with an increase in sedimentary maturity (Fig. 5a). This is also confirmed by  
440  $\text{Al}_2\text{O}_3/\text{TiO}_2$  (20.85 and 22.89) and  $\text{Al}_2\text{O}_3/\text{Na}_2\text{O}$  (13.13 and 10.86) ratios within the range  
441 of those of the PAAS (18.90 and 15.75, respectively).

442

### 443 3.3.2. Source area weathering and recycling

444

445 The average CIA (Chemical Index of Alteration; Nesbitt and Young, 1982) and PIA  
446 (Plagioclase Index of Alteration; Fedo et al., 1995) values for the metasedimentary rocks  
447 from Albarrana Succession (53 and 53, respectively) and Cabril-Peña Grajera Succession  
448 (56 and 60, respectively) indicate relative fresh rocks and low weathering alteration  
449 (Table 2) (Fig. 5b). Both indexes are far below those of the PAAS (CIA=70; PIA=79),

450 and imply a limited secondary conversion of plagioclase/K-feldspars to clay minerals.  
451 Significant K-addition can be excluded in view of the slightly higher K<sub>2</sub>O contents in the  
452 CGS metasedimentary samples (avg. 4.57 wt.%) compared to those of the PAAS (3.7  
453 wt.%), and the very low K<sub>2</sub>O contents of the quartzites from AS (avg. 0.37 wt.%) (Fig.  
454 5b). As expected, this very low K abundance is in agreement with low contents in other  
455 LILE elements (Ba, Rb, and Cs). Low Rb (avg. 11.7 ppm) together with high Sr contents  
456 (avg. 245.3 ppm) in these samples provide very low Rb/Sr ratios (0.05), representing a  
457 low redistribution of the Sr<sup>2+</sup> and Ca<sup>2+</sup>, considering also the high CaO abundances (avg.  
458 1.98 wt.%), and typical Sr abundances for quartz-feldspathic rocks (Mielke, 1979).  
459 However, the slightly high CaO contents suggest that hydrothermal alteration and CaO  
460 gain could be ruled out after considering the low LOI values (0.47 and 1.99 for AS and  
461 CGS, respectively).

462

463 An increase in the chemical maturity is consistent with a higher influence of post-  
464 depositional processes over the terrigenous sediments, as confirmed by PIA values for  
465 Albariza-Bembézar Succession and Azuaga Formation samples (82 and 80, respectively)  
466 (Table 2), which are similar to PAAS (79). This implies certain transformation of  
467 plagioclase/feldspar to clay minerals, in agreement with high Al (20.60 and 18.18 wt.%,  
468 respectively), and low Ca contents (0.48 and 0.58 wt.% CaO, respectively). Values below  
469 1 of the Index of Compositional Variability (ICV; Cox et al., 1995) calculated for the  
470 samples from ABS and AzF (0.7 and 0.8, respectively) imply the presence of clay  
471 minerals dominantly with a recycling character. The relative weathering and post-  
472 sedimentary alteration of these samples are confirmed by average CIA values of 71 for  
473 both units, matching those of the PAAS (70) and indicating a moderate weathering (Fig.

474 5b), as also deduced from high Rb/Sr ratios (1.27 and 1.03, respectively), well beyond  
475 the 0.5 value that McLennan et al. (1993) suggest for a limited chemical alteration.

476

### 477 3.3.3. Rare Earth Elements composition (REE)

478

479 Quartz-feldspathic Albarrana Succession samples show very low bulk REE contents (avg.  
480 8.3; Table 3), as expected from their high quartz contents, the relative lack of REE-  
481 bearing heavy minerals, and the aforementioned small fraction of clay minerals (Taylor  
482 and McLennan, 1988). Their chondrite-normalized REE patterns (Nakamura, 1974; Fig.  
483 6a) are highly influenced by the significant abundance in plagioclase and feldspar (Taylor  
484 and McLennan, 1988; Condie et al., 1995), where the most distinctive features are a  
485 depletion in LREE, a positive trend in HREE ( $Gd_N/Yb_N=0.4$ ), and a highly positive Eu-  
486 anomaly (avg. 4.49), compatible with their high plagioclase fraction and CaO  
487 abundances. Sample ALBA-03 presents higher HREE contents, which combined with a  
488 very high Zr (1113 ppm) and Hf (31.4 ppm) abundances (Fig. 6c), suggest a likely greater  
489 presence of zircon and rutile with low fractionation of the  $TiO_2$ , probably accumulated in  
490 the coarser fraction of the sediment, since these heavy minerals commonly remain inert  
491 through sorting processes (Garcia et al., 1991). By contrast, the bulk REE-abundances in  
492 the metasedimentary samples Cabril-Peña Grajera Succession (290.5), Albariza-  
493 Bembézar Succession (331.7), and Azuaga Formation (231.9) (Table 3) are above those  
494 of the PAAS (184.8), although their chondrite normalized REE patterns are similar (Fig  
495 6a and 6b), sharing typical features with felsic igneous sources with an upper crust  
496 provenance: (i) a significant LREE fractionation over their HREE abundances, with high  
497  $La_N/Yb_N$  ratios (avg. 12.5, 14.5, and 8.5, respectively), (ii) a negative Eu anomaly (0.59,  
498 0.67, and 0.68, respectively) comparable with that of the PAAS (0.65), and finally (iii)

499 almost flat HREE patterns, with  $Gd_N/Yb_N$  values close to unity (1.8, 2.2, and 1.5,  
500 respectively), and slightly higher than those of the PAAS (1.3). The large variation in  
501 LREE for CGS samples (ranging from 74 to 542) (Fig. 6a) is probably because of variable  
502 LREE-bearing mineral content (e.g. monazite), as indicated by the wide range in  
503  $Gd_N/Yb_N$  ratios (from 0.8 to 3.5) (McLennan, 1989; McLennan and Taylor, 1991), with  
504 an average value typical for igneous rocks with an upper crust affinity. While HREE  
505 contents in ABS are controlled by the garnet fraction, zircon is a major factor in HREE  
506 abundances for AzF samples, in agreement with a positive correlation between Zr, Hf and  
507 HREE contents.

508

#### 509 3.3.4. Provenance

510

511 In addition to the above mentioned characteristic REE-patterns similar to the PAAS and  
512 typical in felsic igneous sources with an upper continental crust affinity, numerous  
513 elemental abundances and their ratios suggest dominant felsic contributions for the  
514 metasedimentary rocks of the Sierra Albarrana Group. The  $Al_2O_3/TiO_2$  ratios (on average  
515 for Albarrana, Cabril-Peña Grajera, Albariza-Bembezar Successions and Azuaga  
516 Formation: 30.2, 20.5, 20.9, 22.9, respectively; Table 2) of these two insoluble elements  
517 and usually unaffected by weathering processes show values above those of the PAAS  
518 (18.9), and support the felsic nature of source rocks. Low Cr and Ni contents are even  
519 below the detection limits in the Albarrana Succession quartz-feldspathic samples, and  
520 rule out mafic/ultramafic contributions (Armstrong-Altrin et al., 2004). Very low Cr/V  
521 ratios (0.88, 0.84, and 0.80 for Cabril-Peña Grajera, Albariza-Bembezar Successions and  
522 Azuaga Formation, respectively) (Table 2) and similar to those of the PAAS (0.79)  
523 exclude a mafic/ultramafic source, confirmed by high Y/Ni values, displaying a trend to

524 granitic end-members compositions, with an absence of mafic/ultramafic detritus  
525 (Hiscott, 1984; McLennan et al., 1993) (Fig. 7a). Relatively high La (avg. 64.2, 71.8, and  
526 46.4 ppm, respectively) and Th (avg. 18.9, 22.3, and 18.8 ppm, respectively) abundances  
527 found in CGS, ABS, and AzF samples, compared to those of the PAAS (38.0 and 14.6  
528 ppm, respectively) are in agreement with a felsic affinity. Therefore, the comparison  
529 between these two latter immobile elements with those commonly associated with  
530 mafic/ultramafic source rocks (Sc, Cr and Co), yields very low Sc/Th (avg. 0.78, 0.74,  
531 and 0.84 for CGS, ABS, and AzF, respectively) and Cr/Th (avg. 4.19, 4.01, and 4.30,  
532 respectively) ratios, lower than those of the PAAS (1.10, and 7.53, respectively), and  
533 within the range of felsic rocks (Cox et al., 1995; Cullers, 2002; McLennan et al., 2006)  
534 (Fig. 7b). Likewise Cr/Th and Eu/Eu\* values (Table 2 and Table 3) fit those proposed by  
535 Cullers (1994) (2.5–17.5 and 0.48–0.78, respectively) for sediments sourced from felsic  
536 rocks. The La/Sc vs. Co/Th diagram (Fig. 8a) places the Sierra Albarrana  
537 metasedimentary rocks close to the PAAS and to typical values for felsic volcanic rocks,  
538 and far from the common Co/Th and La/Sc values in basaltic and andesitic sources. Felsic  
539 volcanic rocks represent an important terrigenous contribution in post-Archean  
540 continental arc systems (Condie et al., 1993). In differentiating specific felsic volcanic  
541 compositions, the Nb/Y vs Zr/Ti diagram in Figure 8b shows that most of the samples  
542 plot in the rhyodacite/dacite composition field, following the Rhyolitic/dacitic trend  
543 (Winchester and Floyd, 1977; Fralick and Kronberg, 1997).

544

### 545 3.3.5. Tectonic setting

546

547 A set of PAAS-normalised major and trace elements diagrams from three units described  
548 in Sierra Albarrana Group are presented in Figure 9, with the exception of the three

549 quartz-feldspathic samples from the Albarrana Succession, whose abundances represent  
550 an almost widespread compositional depletion related to PAAS (Fig. 6c). The patterns  
551 displayed by the three units match those proposed by Winchester and Max (1989) for  
552 passive continental margins (Fig. 9), and also match those found in Early Cambrian shales  
553 (slates) from the autochthonous section in the southern Central Iberian Zone (Pusa Gp;  
554 Fuenlabrada et al., 2016) and in Middle Cambrian metapelitic rocks from the NW Basal  
555 Allochthonous Units (Fuenlabrada et al., 2012). Both are indicative of an upper  
556 continental crust provenance, whose sedimentation was influenced by the earlier stages  
557 of a Cambrian-Ordovician passive margin (Pieren Pidal, 2000; Díez Fernández et al.,  
558 2010; Fuenlabrada et al., 2020). They show an average geochemical composition similar  
559 to PAAS, with the majority of the normalized major and trace elements close to unity,  
560 with no evident depletion in LILE elements, and negative anomalies in different  
561 proportions in the case of Sr, P, and Ti abundances (Fig. 9). They all suggest an important  
562 influence of the sedimentary processes over the terrigenous sediments, as a result of  
563 distant source areas and effective recycling processes. This is confirmed by Th/U ratios  
564 (avg. 7.6, 4.4, 4.8, and 4.7 for AS, CGU, ABU, and AzU, respectively) around those of  
565 PAAS (4.7), and above typical values for sedimentary rocks sourced from crustal igneous  
566 rocks with cratonic provenance (3.5-4.0; McLennan et al., 1993).

567

568 The geochemistry of the metasedimentary rocks from Sierra Albarrana Group is  
569 compatible with deposition in a peri-continental section influenced by a continental active  
570 margin that evolved to a more stable environment (passive margin?) during Early  
571 Cambrian times. The La/Th versus Hf diagram (Fig. 10a) shows some affinity for acidic  
572 arc sources, some samples having similar values to those of the PAAS (average value for  
573 upper continental crust). However, the majority of the samples displays an evident trend

574 to higher Hf contents, which according to Floyd and Leveridge (1987) could be  
575 consequence of the erosion effect of a continental basement with increasingly older  
576 metasedimentary rocks. Such trend in the denudation process could explain the increase  
577 in maturity observed in the Sierra Albarrana Group, with a progressive release of zircon  
578 and other accessory, but highly stable minerals and the subsequent enrichment in Zr and  
579 Hf that is typical for passive margin sediments (Bhatia and Crook, 1986; McLennan et  
580 al., 1993). Supporting the latter idea, the Th/Sc and Zr/Sc ratios (Table 2) (Fig. 10b) show  
581 values that suggest sorting and recycling to some extent, what fits with passive margin  
582 turbidites better than with sediments related to an active arc, which would follow normal  
583 geochemical compositional variations and limited recycling (McLennan et al., 1993; Cox  
584 et al., 1995) (Fig. 10b).

585

#### 586 3.3.6. Sm-Nd isotopes

587

588 The Sm-Nd isotope data for the Sierra Albarrana metasedimentary rocks are given in  
589 Table 4 and Figure 11. An Early Cambrian maximum depositional age (ca. 530 Ma) has  
590 been selected for  $\epsilon\text{Nd}_{(i)}$  calculations. No significant variation is observed in the whole  
591 group of samples, which defines a single Nd-isotope population. Relatively similar  
592  $^{143}\text{Nd}/^{144}\text{Nd}$  initial ratios, ranging from 0.51138 to 0.51172, suggest a likely common  
593 source for all of them. Their  $^{147}\text{Sm}/^{144}\text{Nd}$  ratios (from 0.1092 to 0.1287) are similar to  
594 those of continental crust ( $\sim 0.12$ ; DePaolo, 1983), and always below the limit  
595 ( $^{147}\text{Sm}/^{144}\text{Nd} = 0.165$ ), defined by Stern (2002) for reliable Nd model age calculations,  
596 sharing typical values among clastic sediments (0.1 to 0.13; Zhao et al., 1992). They show  
597 relatively uniform  $\epsilon\text{Nd}_{(0)}$  values (from -17.1 to -10.3; Table 4) and negative  $\epsilon\text{Nd}_{(530)}$   
598 values, varying between -11.3 and -4.5 (Fig. 11). Nd TDM model ages were calculated



599 according to DePaolo (1991), yielding Late Paleoproterozoic to Early Mesoproterozoic  
600 ages (1388 – 1897 Ma), with an average value at 1721 Ma, similar to those already  
601 published by López-Guijarro et al. (2008).

602

603 **4. Discussion: type of basin model in which the Sierra Albarrana Group was**  
604 **deposited**

605

606 The quite negative  $\epsilon\text{Nd}_{(530)}$  values (from -11.3 to -4.5; Table 4) calculated for the  
607 metasedimentary series of the Sierra Albarrana Group indicate a dominant input of  
608 terrigenous materials with an old continental crust affinity and limited contributions from  
609 juvenile sources. The geochemical compositions place the deposition in a continental  
610 active margin. Given the significant and increasing influence of the sedimentary  
611 processes and transport over the pelitic protoliths, and the recycled character of the  
612 terrigenous sediments, the conditions would have probably evolved to those of a passive  
613 margin. Both  $\epsilon\text{Nd}_{(530)}$  and  $f^{\text{Sm/Nd}}$  values (from -0.445 to -0.346; Table 4) are compatible  
614 with those proposed by McLennan and Hemming (1992) for sedimentary rocks deposited  
615 in tectonic settings sharing continental active margin and passive margin/cratonic  
616 features. The geochemical composition of our samples (Fig. 9 and 10) points to the same  
617 direction. The negative  $\epsilon\text{Nd}_{(530)}$  and geochemical features such as Th/U, Th/Sc, and  
618 Eu/Eu\*, account for a significant sedimentary maturity and recycled character  
619 (McLennan et al., 1993), favouring a provenance from old and reworked continental  
620 upper crust materials with an evident felsic contribution. The metasedimentary rocks from  
621 Sierra Albarrana Group display uniform Sm/Nd ratios, which suggests an intense  
622 recycling history and a limited contribution from differentiated sources. These samples  
623 show Nd-isotope features quite different from those found in typical arc-related rocks,

624 with variable Sm/Nd ratios and positive  $\epsilon\text{Nd}$  (e.g. metasedimentary series in the NW  
625 Upper Allochthonous Units; Fuenlabrada et al., 2010, 2020). As mentioned before, the  
626 rest of geochemical proxies indicate a reworking of detrital materials with a high  
627 influence of the sedimentary transport, and likely linked to a continental active margin or  
628 an incipient passive margin. This is also confirmed by the comparison with a wide range  
629 of geochemical indicators used by Bhatia and Crook, 1986, to constrain the affinity with  
630 certain geodynamic scenarios. Considering Nd model ages in siliciclastic rocks as a  
631 weighted average of contributions with a different age and provenance, potentially  
632 derived from nearby surrounding source areas and/or, according to some authors areas  
633 located thousands of kilometres away (e.g. Avigad et al., 2003; Morag et al., 2011), the  
634 here presented very old Nd model ages (avg. 1721 Ma; Table 4 and Fig. 11) account for  
635 a limited and variable mixing with juvenile detrital materials coming from the outermost  
636 part of the active margin and magmatic arc sources, and suggest a dominant input from  
637 older basement sections. The closeness of the paleobasins of the Ediacaran sedimentary  
638 sequences from the Serie Negra Group to the Cadomian magmatic arc define specific and  
639 identifiable geochemical features (Rojo-Pérez et al., 2019 and submitted), although their  
640 Nd model ages do not mirror significant juvenile contributions from the magmatic  
641 activity, with constant and old TDM ages with an old crustal affinity from a Cadomian  
642 basement provenance (Rojo-Pérez et al., submitted). The geochemical and isotope data  
643 here presented for the Sierra Albarrana Group suggest that their sedimentary protoliths  
644 were not laid down coevally with ongoing magmatism, at least not close to a magmatic  
645 axis, since there is no geochemical evidence for a significant influence of the arc-system  
646 over the geochemical features in the whole group of rocks from Sierra Albarrana. In this  
647 regard, the recycling of an old (Paleoproterozoic) basement into newly-formed igneous  
648 rocks that were eroded from the arc-system should be considered a rather minor

649 contributor, unlike what might have happened with the coeval Ediacaran-Cambrian  
650 Malcocinado volcanoclastic series, with Nd-isotope features more in line with a greater  
651 influence of the magmatic activity of the Cadomian arc (López-Guijarro et al., 2008). All  
652 these geochemical and isotopic characteristics match those found in the Early Cambrian  
653 sedimentary sequences of the autochthonous section of the Central Iberian Zone (Pusa  
654 shales Formation – Upper Unit), which show, in average values, slightly less negative  
655  $\epsilon\text{Nd}_{(530)}$  (from -5.2 to -4.0) and younger TDM model ages (1444-1657 Ma; Fuenlabrada  
656 et al., 2016), although overlapping some individual values obtained in the autochthonous  
657 section of the Sierra Albarrana Group (Fig. 11). Homogeneous geochemical data of the  
658 Early Cambrian sedimentary sequences in Central Iberian Zone also support a high  
659 textural and mineralogical maturity compatible with old crustal materials, probably  
660 coming from a reworked continental source in an emerged Gondwanan hinterland  
661 location (Fuenlabrada et al., 2016). The Paleoproterozoic and Mesoproterozoic TDM  
662 model ages (Fig. 11) probably result from a mixing of limited Neoproterozoic and  
663 dominant Paleoproterozoic/Archean components, pointing to the denudation of an old  
664 continental crust (Paleoproterozoic basement), or a crust built at the expense of it, that  
665 was exposed during Early Cambrian times. This is compatible with an exposure of a  
666 Paleoproterozoic basement (e.g., in the Moroccan Meseta; Pereira et al., 2015b) and/or  
667 erosion of old recycled continental crust. The increase in weathering indexes (CIA and  
668 PIA values; Table 2) in the metasedimentary rocks of the Albarrana Succession through  
669 to the Azuaga Formation is compatible with both possibilities.

670

671 Although our results are in agreement with those obtained by Lopez-Guijarro et al.  
672 (2008), who suggested common Archean/Paleoproterozoic old continental crust sources  
673 for the Serie Negra Group and the metasedimentary rocks of Sierra Albarrana during the

674 latest Neoproterozoic, a Cambrian age for the sedimentary sequences of the Sierra  
675 Albarrana Group precludes a direct comparison with the Ediacaran Serie Negra Group.  
676 The most probable contributor for the detrital material was a Paleoproterozoic basement  
677 and/or an old recycled continental crust currently located in more eastern sections of the  
678 Gondwanan margin than those of the Serie Negra. The Tuareg Shield (Fig. 12b) shows  
679 abundant Paleoproterozoic and Archean source rocks with scarce Neoproterozoic and  
680 Mesoproterozoic ages (Brahimi et al., 2018), being probably the dominant contributor,  
681 through the Saharan platform, as previously suggested by Cambeses et al. (2017). These  
682 old recycled materials present Nd-isotope features comparable with those of the southern  
683 Central Iberian Zone (Fuenlabrada et al., 2016, 2020), what suggests easternmost  
684 locations for the Variscan autochthonous sections of the Iberian Massif (Bea et al., 2010;  
685 Talavera et al., 2013; Fernández-Suárez et al., 2014) (Fig. 12b).

686

687 Recent paleogeographic reconstructions of the peri-Gondwanan domain acknowledge  
688 that the autochthonous sections of the Variscan Orogen occupied inward positions across  
689 the margin of Gondwana relative to their respective allochthons (Díez Fernández et al.,  
690 2016). This reconstruction fits well with the orogen-scale distribution of paleogeographic  
691 domains of the Cadomian arc-system during the latest Ediacaran and Cambrian. The most  
692 external sections of the Cadomian arc-system, such as the fore-arc and arc, are preserved  
693 in the Variscan Upper Allochthon (Andonaegui et al., 2002; Díaz García et al., 2010;  
694 Fuenlabrada et al., 2010; Albert et al., 2015). The Variscan Ophiolitic and Basal  
695 allochthons include remnants of a Cadomian back-arc (Abati et al., 2010; Díez Fernández  
696 et al., 2010, 2016; Fuenlabrada et al., 2012; Andonaegui et al., 2017; Arenas et al., 2018,  
697 2020; Sánchez Martínez et al., 2020), while in the autochthon were accumulated thick  
698 sedimentary series in the flank of that back-arc basin closer to the mainland in a

699 differentiated lateral position (Rodríguez Alonso et al., 2004b; Pereira et al., 2012a;  
700 Fuenlabrada et al., 2016, 2020). Variscan subduction/accretion polarity for the peri-  
701 Gondwanan terranes of Iberia was directed toward Laurussia (i.e. to the W and SW in  
702 present-day coordinates; Díez Fernández et al., 2016). Therefore, the current  
703 juxtaposition of Variscan allochthons on top of autochthons could be roughly translated  
704 in paleogeographic terms into a more internal position across the margin as we move  
705 down through the Variscan tectonic pile, and also as we move E or NE through the same  
706 allochthonous or autochthonous terrane. Accordingly, the position of the Sierra Albarrana  
707 Group to the SW of the Variscan autochthon widely exposed in the Central Iberian Zone  
708 would imply a position closer to the mainland for the latter, in a more eastern lateral  
709 location along the Gondwanan margin, closer to the Sahara Metacraton (Fig. 12b) (Bea  
710 et al., 2010; Talavera et al., 2012; Kromer and Romer, 2013; Fernández-Suárez et al.,  
711 2014; Albert et al., 2015; Stephan et al., 2019b; Fuenlabrada et al., 2020).

712

713 Given the widespread angular unconformity between Ediacaran and Early Cambrian  
714 rocks that can be recognized across the Iberian Massif, topographic uplift must have  
715 played a role in the onset of Early Cambrian basins across the margin. Ediacaran thrusting  
716 (obduction) directed toward mainland Gondwana was responsible for the emplacement  
717 of peripheral (fore-arc) sections of the arc-system onto inboard sections of the Gondwana  
718 margin (Díez Fernández et al., 2019), which came along with coeval inversion (inland-  
719 verging folds; Díaz García, 2006) and across-margin segmentation (Villaseca et al., 2014)  
720 of back-arc Cadomian basins. Inland-directed obduction of peripheral sections of an arc-  
721 system together with inland-verging folds in the back-arc are strongly compatible with  
722 the development of a retro-arc (retro-foreland) basin over the back of the arc-system (Fig.  
723 12a). In a convergent scenario, the interaction between the peri-Gondwanan trench and

724 the external part of the continent during Neoproterozoic times resulted in widespread  
725 contraction (Díez Fernández et al., 2019), thus generating significant relief, either at the  
726 expense of the fore-arc, arc, or even the back-arc, which would have been the main  
727 detritus suppliers for a retro-arc basin. The more external Ediacaran-Cambrian  
728 paleoposition of the Variscan autochthonous section that is preserved in Sierra Albarrana  
729 relative to the rest of the Variscan autochthon that is preserved elsewhere to the N and  
730 NW, makes the Sierra Albarrana Group a good candidate to represent the infilling of a  
731 Cambrian retro-arc basin fed by detritus coming from tectonically uplifted sections of the  
732 arc and fore-arc, as this would be a domain of the Ediacaran back-arc of the autochthon  
733 rather close to the uplifted sections. All the geochemical features of those sequences  
734 presented in this work are fully compatible with this interpretation.

735

736 The distribution of siliciclastic materials within the Sierra Albarrana sedimentary basin  
737 follows predictable models for the evolution in foreland basins, where the sedimentary  
738 sequences record long-term climatic and tectonic changes (Armitage et al., 2011). The  
739 presence of *Skolithos*, *Monocraterion*, and *Arenicolites* in the Albarrana Succession  
740 indicates a shallow marine environment for the deposition of this series (Azor et al.,  
741 1991), possibly in a bulge section. In the Cabril-Peña Grajera and Albariza-Bembézar  
742 successions, the flysch-type deposits, with relatively immature sediments and turbiditic  
743 character, could be the result of deepening in the retro-arc basin, possibly related to  
744 tectonically-induced subsidence in a fore-deep section. The greater influence of the  
745 sedimentary transport, as suggested by the increase in the geochemical maturity and  
746 recycling character of the metasedimentary record in the Albariza-Bembézar Succession  
747 and Azuaga Formation could be related to a widening of the basin, what would have  
748 heralded the terminal stages of contraction in the upper plate, where the continuous input

749 of recycled sediments from old basement sources filled the basin in a more stable  
750 environment such as is the case of the intertidal zone deposits in a marine platform  
751 suggested for the Azuaga Formation (Insúa et al., 1990; González del Tánago, 1995; and  
752 references therein).

753

## 754 **5. Main conclusions**

755

756 Nd-isotope data from metasedimentary series of the Sierra Albarrana Group (SW Iberian  
757 Autochthonous Domain) are compatible with old reworked materials with continental  
758 crust affinity and limited contributions from juvenile sources. This, together with a high  
759 recycling character of the terrigenous sediments place the basins within an active margin  
760 sharing geochemical features with the initial stages of a passive margin. The geochemical  
761 and isotopic features of the Sierra Albarrana Group are similar to those found in the  
762 sedimentary sequences of the autochthonous section of the Central Iberian Zone, which  
763 implies a comparable depositional setting during their sedimentation in Early Paleozoic  
764 times and a close paleolocation of their sedimentary basins, but in an easternmost location  
765 along the Gondwanan margin (Tuareg Shield – Sahara Metacraton). The progressive  
766 denudation of a Paleoproterozoic basement or a recycled continental crust was the  
767 dominant source for the recycled materials with old Nd model ages found in the  
768 metasedimentary sequences in Sierra Albarrana. The exposure of this old crustal section  
769 after topographic uplift was caused by an Ediacaran inland-directed thrusting, which  
770 emplaced fore-arc sections of the arc-system onto inboard sections of the Gondwanan  
771 margin. This contractive scenario during latest Neoproterozoic times caused that these  
772 uplifted arc and fore-arc sections were the dominant detrital contributors for the filling of

773 a retro-arc basin, which is considered as the most probable setting for the deposit of the  
774 Sierra Albarrana sedimentary rocks in Early Cambrian times.

775

## 776 **6. Acknowledgements**

777

778 This work is dedicated to the extensive career that Professor Carmen Galindo devoted to  
779 Geology, and more particularly to Isotope Geochemistry, carrying out for over 25 years  
780 an invaluable work as head of the Geochronology and Isotope Geochemistry Service  
781 (Universidad Complutense de Madrid). She was also an inspiration to Geology students  
782 who decided devote their scientific career to the fascinating field of Geochemistry. We  
783 would like to acknowledge the invaluable help of the editor Pilar Montero, as well as the  
784 insightful and constructive contributions made by Aitor Cambeses and another  
785 anonymous reviewer that has resulted in an improved version of the manuscript. Financial  
786 support has been provided by the Spanish project CGL2016-76438-P (Ministerio de  
787 Economía Industria y Competitividad). This work is a contribution to IGCP project 683  
788 (Pre-Atlantic geological connections among northwest Africa, Iberia and eastern North  
789 America: Implications for continental configurations and economic resources).

790

## 791 **7. References**

792

793 Ábalos, B., Eguiluz, L., Apalategui, O., (1990). Constitución tectono-estratigráfica del  
794 Corredor Blastomilonítico de Badajoz - Córdoba: nueva propuesta de subdivisión.  
795 Geogaceta 7, 71-73.

796



797 Ábalos, B., Gil Ibarguchi, J.I., Sánchez-Lorda, M.E., Paquette, J.L., (2012).  
798 African/Amazonian Proterozoic correlations of Iberia: a detrital zircon U-Pb study of  
799 early Cambrian conglomerates from the Sierra de la Demanda (northern Spain). *Tectonics*  
800 31 TC3003. <https://doi.org/10.1029/2011TC003041>  
801  
802 Abati, J., Gerdes, A., Fernández-Suárez, J., Arenas, R., Whitehouse, M.J., Díez  
803 Fernández, R., (2010). Magmatism and early-Variscan continental subduction in the  
804 northern Gondwana margin recorded in zircons from the basal units of Galicia, NW  
805 Spain. *Geological Society of America Bulletin*. 122, 219–235.  
806 <https://doi.org/10.1130/B26572.1>  
807  
808 Abati, J., Arenas, R., Díez Fernández, R., Albert, R., Gerdes, A., (2018). Combined zircon  
809 U-Pb and Lu-Hf isotopes study of magmatism and high-P metamorphism of the basal  
810 allochthonous units in the SW Iberian Massif (Ossa-Morena complex). *Lithos* 322, 20–  
811 37.  
812  
813 Abbo, A., Avigad, D., Gerdes, A., Güngör, T., (2015). Cadomian basement and Paleozoic  
814 to Triassic siliciclastics of the Taurides (Karacahisar dome, south-central Turkey):  
815 paleogeographic constraints from U–Pb–Hf in zircons. *Lithos* 227, 122–139.  
816 <https://doi.org/10.1016/j.lithos.2015.03.023>  
817  
818 Alvarez Nava, H., García Casquero, J.L., Gil Toja, A., Hernández Urroz, J., Lorenzo  
819 Alvarez, S., López Díaz, F., Mira López, M., Monteserín, V., Nozal, F., Pardo, M.V.,  
820 Picart, J., Robles, R., Santamaría, J., Sole, F.J., (1988). Unidades litoestratigráficas de los

821 materiales Precámbrico-Cámbricos en la mitad suroriental de la Zona Centro-Ibérica. In:  
822 II Congreso Geológico de España, SGE, Granada. 1. pp. 19–22.  
823  
824 Albert, R., Arenas, R., Gerdes, A., Sánchez Martínez, S., Fernández-Suárez, J.,  
825 Fuenlabrada, J.M., (2015). Provenance of the Variscan Upper Allochthon (Cabo Ortegal  
826 complex, NW Iberian Massif). *Gondwana Research*. 28, 1434–1448.  
827 <https://doi.org/10.1016/j.gr.2014.10.016>  
828  
829 Andonaegui, P., González del Tánago, J., Arenas, R., Abati, J., Martínez Catalán, J.R.,  
830 Peinado, M., Díaz García, F., (2002). In: Martínez Catalán, J.R., Hatcher, R.D., Arenas,  
831 R., Díaz García, F. (Eds.), *Tectonic setting of the Monte Castelo gabbro (Ordenes*  
832 *Complex, northwestern Iberian Massif): evidence for an arc-related terrane in the hanging*  
833 *wall to the Variscan suture*. 364. *Variscan-Appalachian Dynamics: The Building of the*  
834 *Late Paleozoic Basement*. Geological Society of America, Special Paper, pp. 37–56.  
835 <https://doi.org/10.1130/0-8137-2364-7.37>  
836  
837 Andonaegui, P., Arenas, R., Albert, R., Sánchez Martínez, S., Díez Fernández, R.,  
838 Gerdes, A., (2016). The last stages of the Avalonian–Cadomian arc in NW Iberian Massif:  
839 isotopic and igneous record for a long-lived peri-Gondwanan magmatic arc.  
840 *Tectonophysics* 681, 6–14. <https://doi.org/10.1016/j.tecto.2016.02.032>  
841  
842 Andonaegui, P., Abati, J., Díez Fernández, R., (2017). Late Cambrian magmatic arc  
843 activity in peri-Gondwana: geochemical evidence from metagranitoid rocks of the Basal  
844 Allochthonous Units of NW Iberia. *Geologica Acta* 15 (4), 305–321.  
845 <https://doi.org/10.1344/GeologicaActa2017.15.4.4>

846

847 Apalategui, O., Borrero, J., Higuera, P., (1985). División en grupos de rocas en Sierra  
848 Morena Oriental. Colección Temas Geológico-Mineros, 2: 73-80.

849

850 Arenas, R., Gil Ibarra, J.I., González Lodeiro, F., Klein, E., Martínez Catalán, J.R.,  
851 Ortega Gironés, E., Pablo Maciá, J.G.d., Peinado, M., (1986). Tectonostratigraphic units  
852 in the complexes with mafic and related rocks of the NW of the Iberian Massif. *Hercynica*  
853 2, 87–110.

854

855 Arenas, R., Díez Fernández, R., Sánchez Martínez, S., Gerdes, A., Fernández-Suárez, J.,  
856 Albert, R., (2014). Two-stage collision: exploring the birth of Pangea in the Variscan  
857 terranes. *Gondwana Research*. 25, 756–763. <https://doi.org/10.1016/j.gr.2013.08.009>

858

859 Arenas, R., Sánchez Martínez, S., Díez Fernández, R., Gerdes, A., Abati, J., Fernández-  
860 Suárez, J., Andonaegui, P., González Cuadra, P., López Carmona, A., Albert, R.,  
861 Fuenlabrada, J.M., Rubio Pascual, F.J., (2016a). Allochthonous terranes involved in the  
862 Variscan suture of NW Iberia: a review of their origin and tectonothermal evolution.  
863 *Earth-Science Reviews* 161, 140–178. <https://doi.org/10.1016/j.earscirev.2016.08.010>

864

865 Arenas, R., Díez Fernández, R., Rubio Pascual, F.J., Sánchez Martínez, S., Martín Parra,  
866 L.M., Matas, J., González del Tánago, J., Jiménez-Díaz, A., Fuenlabrada, J.M.,  
867 Andonaegui, P., García-Casco, A., (2016b). The Galicia – Ossa-Morena zone: proposal  
868 for a new zone of the Iberian Massif. Variscan implications. *Tectonophysics* 681, 135–  
869 143. <https://doi.org/10.1016/j.tecto.2016.02.030>

870

871 Arenas, R., Fernández-Suárez, J., Montero, P., Díez Fernández, R., Andonaegui, P.,  
872 Sánchez Martínez, S., Albert, R., Fuenlabrada, J.M., Matas, J., Martín Parra, L.M., Rubio  
873 Pascual, F.J., Jiménez-Díaz, A., Pereira, M.F., (2018). The Calzadilla Ophiolite (SW  
874 Iberia) and the Ediacaran fore-arc evolution of the African margin of Gondwana.  
875 *Gondwana Research*. 58, 71–86. <https://doi.org/10.1016/j.gr.2018.01.015>  
876

877 Arenas, R., Sánchez Martínez, S., Albert, R., Haissen, F., Fernández-Suárez, J., Pujol-  
878 Solà, N., Andonaegui, P., Díez Fernández, R., Proenza, J.A., García-Casco, A., Gerdes,  
879 A., (2020). 100 myr cycles of oceanic lithosphere generation in peri-Gondwana:  
880 Neoproterozoic–Devonian ophiolites from the NW African–Iberian margin of Gondwana  
881 and the Variscan Orogen. *Geological Society, London, Special Publications*, 503.  
882 <https://doi.org/10.1144/SP503-2020-3>  
883

884 Armitage, J., Duller, R., Whittaker, A. Allen, P.A., (2011). Transformation of tectonic  
885 and climatic signals from source to sedimentary archive. *Nature Geoscience* 4, 231–235.  
886 <https://doi.org/10.1038/ngeo1087>  
887

888 Armstrong-Altrin, J.S., Lee, Y.I., Verma, S.P., Ramasamy, S., (2004). Geochemistry of  
889 sandstones from the upper Miocene Kudankulam formation, southern India: Implications  
890 for provenance, weathering, and tectonic setting. *Journal of Sedimentary Research* 74,  
891 285–297. <https://doi.org/10.1306/082803740285>  
892

893 Avigad, D., Kolodner, K., McWilliams, M., Persing, H., Weissbrod, T., (2003). Origin of  
894 northern Gondwana Cambrian sandstone revealed by detrital zircon SHRIMP dating.  
895 *Geology* 31 (3), 227–230.

896 [https://doi.org/10.1130/0091-7613\(2003\)031<0227:OONGCS>2.0.CO;2](https://doi.org/10.1130/0091-7613(2003)031<0227:OONGCS>2.0.CO;2)  
897  
898 Avigad, D., Gerdes, A., Morag, N., Bechstädt, T., (2012). Coupled U–Pb–Hf of detrital  
899 zircons of Cambrian sandstones from Morocco and Sardinia: Implications for provenance  
900 and Precambrian crustal evolution of North Africa. *Gondwana Research*. 21, 690–703.  
901 <https://doi.org/10.1016/j.gr.2011.06.005>  
902  
903 Avigad, D., Rossi, Ph., Gerdes, A., Abbo, A., (2018). Cadomian metasediments and  
904 Ordovician sandstone from Corsica: detrital zircon U–Pb–Hf constrains on their  
905 provenance and paleogeography. *International Journal of Earth Sciences (Geol.*  
906 *Rundsch.)* 107, 2803–2818. <https://doi.org/10.1007/s00531-018-1629-3>  
907  
908 Azor, A., (1994). Evolución tectonometamórfica del límite entre las zonas Centroibérica  
909 y de Ossa-Morena (Cordillera Varisca, SO de España) (PhD thesis) Universidad de  
910 Granada, Spain (295 pp).  
911  
912 Azor, A., Ballèvre, M., (1997). Low-Pressure Metamorphism in the Sierra Albarrana  
913 Area (Variscan Belt, Iberian Massif). *Journal of Petrology* 38 (1), 35-64.  
914 <https://doi.org/10.1093/petroj/38.1.35>  
915  
916 Azor, A., González Lodeiro, F., Marcos, A., Simancas, J.F., (1991). Edad y estructura de  
917 las rocas de Sierra Albarrana (SW del Macizo Hespérico). Implicaciones regionales.  
918 *Geogaceta* 10, 119-124.  
919

920 Azor, A., Lodeiro, F.G., Simancas, J.F., (1994). Tectonic evolution of the boundary  
921 between the central Iberian and the Ossa-Morena zones (Variscan belt, southwest Spain).  
922 *Tectonics* 13, 45–61. doi: 10.1029/93TC02724  
923

924 Azor, A., Expósito, I., González Lodeiro, F., Simancas, J.F., Martínez Poyatos, D.,  
925 (2004). La Unidad de Sierra Albarrana. In Vera, J.A. (ed.), *Geología de España*, SGE-  
926 IGME, Madrid, 182-186.  
927

928 Azor, A., Simancas, J.F., Martínez Poyatos, D.J., Montero, P., González Lodeiro, F.,  
929 Gabites, J., (2012). Nuevos datos geocronológicos sobre la evolución tectonometamórfica  
930 de la Unidad de Sierra Albarrana (Zona de Ossa-Morena, SO de Iberia). *Geo-Temas* 13,  
931 341-344.  
932

933 Azor, A., Simancas, J.F., Martínez Poyatos, D.J., Montero, P., González Lodeiro, F.,  
934 Pérez-Cáceres, I., (2016). U-Pb zircon age and tectonic meaning of the Cardenchosa  
935 pluton (Ossa-Morena Zone). *Geo-Temas* 2, 23–26  
936

937 Ballèvre, M., Le Goff, E., Hébert, R., (2001). The tectonothermal evolution of the  
938 Cadomian belt of northern Brittany, France: a Neoproterozoic volcanic arc.  
939 *Tectonophysics* 331 (1-2), 19–43. [https://doi.org/10.1016/S0040-1951\(00\)00234-1](https://doi.org/10.1016/S0040-1951(00)00234-1)  
940

941 Bandrés, A., (2001). Evolución geodinámica poliorogénica de los dominios  
942 septentrionales de la ZOM. Universidad del País Vasco, pp. 377 Tesis Doctoral.  
943

944 Bea, F., Montero, P., Talavera, C., Abu Anbar, M., Scarrow, J., Molina, J.F., Moreno,  
945 J.A., (2010). The palaeogeographic position of Central Iberia in Gondwana during the  
946 Ordovician: evidence from zircon geochronology and Nd isotopes. *Terra Nova* 22, 341–  
947 346. <https://doi.org/10.1111/j.1365-3121.2010.00957.x>  
948  
949 Bhatia, M.R., Crook, K.A.W., (1986). Trace element characteristics of graywackes and  
950 tectonic setting discrimination of sedimentary basins. *Contributions to Mineralogy and*  
951 *Petrology* 92, 181–193. <https://doi.org/10.1007/BF00375292>  
952  
953 Brahimi, S., Liégeois, J.P., Ghienne, J.F., Munsch, M., Bourmatte, A., (2018). The  
954 Tuareg shield terranes revisited and extended towards the northern Gondwana margin:  
955 Magnetic and gravimetric constraints. *Earth-Science Reviews* 185, 572-599,  
956 <https://doi.org/10.1016/j.earscirev.2018.07.002>  
957  
958 Cambeses, A., Scarrow, J.H., Montero, P., Lázaro, C., Bea, F., (2017). Palaeogeography  
959 and crustal evolution of the Ossa-Morena Zone, southwest Iberia, and the North  
960 Gondwana margin during the Cambro-Ordovician: a review of isotopic evidence.  
961 *International Geology Review* 59, 94–130.  
962 <https://doi.org/10.1080/00206814.2016.1219279>  
963  
964 Carvalhosa, A., (1965). Contribuição para o conhecimento geológico da região entre  
965 Portel e Ficalho (Alentejo). *Memórias dos Serviços Geológicos de Portugal. Nova Série*  
966 11, 1–32.  
967

968 Chacón, J.; Delgado Quesada, M., Garrote, A., (1974). Sobre la existencia de dos  
969 diferentes dominios de metamorfismo regional en la banda Elvas-Badajoz-Córdoba.  
970 Boletín Geológico y Minero 85, pp. 713-717.  
971

972 Collett, S., Schulmann, K., Štípská, P., Míková, J., (2020). Chronological and  
973 geochemical constraints on the pre-variscan tectonic history of the Erzgebirge,  
974 Saxothuringian Zone, Gondwana Research 79, 27-48.  
975 <https://doi.org/10.1016/j.gr.2019.09.009>  
976

977 Condie, K.C., (1993). Chemical composition and evolution of the upper continental crust:  
978 contrasting results from surface samples and shales. Chemical Geology 104, 1–37.  
979 [http://dx.doi.org/10.1016/0009-2541\(93\)90140-E](http://dx.doi.org/10.1016/0009-2541(93)90140-E)  
980

981 Condie, K.C., Dengate, J., Cullers, R.L., (1995). Behavior of rare earth elements in a  
982 paleoweathering profile on granodiorite in the Front Range, Colorado, USA. Geochimica  
983 et Cosmochimica Acta 59 (2), 279-294.  
984 [https://doi.org/10.1016/0016-7037\(94\)00280-Y](https://doi.org/10.1016/0016-7037(94)00280-Y)  
985

986 Cox, R., Lowe, D.R., Cullers, R.L., (1995). The influence of sediment recycling and  
987 basement composition on evolution of mudrock chemistry in the southwestern, United  
988 States. Geochimica et Cosmochimica Acta 59 (14), 2919–2940.  
989 [https://doi.org/10.1016/0016-7037\(95\)00185-9](https://doi.org/10.1016/0016-7037(95)00185-9)  
990

991 Cullers, R.L., (1994). The controls on the major and trace element variation of shales,  
992 siltstones and sandstones of Pennsylvanian–Permian age from uplifted continental blocks



993 in Colorado to platform sediment in Kansas, USA. *Geochimica et Cosmochimica Acta*  
994 58, 4955–4972. [https://doi.org/10.1016/0016-7037\(94\)90224-0](https://doi.org/10.1016/0016-7037(94)90224-0)  
995  
996 Cullers, R.L., (2002). Implications of elemental concentrations for provenance, redox  
997 conditions, and metamorphic studies of shales and limestones near Pueblo, CO, USA.  
998 *Chemical Geology* 191, 305–327. [https://doi.org/10.1016/S0009-2541\(02\)00133-X](https://doi.org/10.1016/S0009-2541(02)00133-X)  
999  
1000 Dallmeyer, R.D., Quesada, C., (1992). Cadomian vs. Variscan evolution of the Ossa-  
1001 Morena zone (SW Iberia): field and  $^{40}\text{Ar}/^{39}\text{Ar}$  mineral age constrains. *Tectonophysics*  
1002 216, 339-364. [https://doi.org/10.1016/0040-1951\(92\)90405-U](https://doi.org/10.1016/0040-1951(92)90405-U)  
1003  
1004 Dallmeyer, R.D., Martínez Catalán, J.R., Arenas, R., Gil Ibarguchi, J.I., Gutiérrez Alonso,  
1005 G., Farias, P., Bastida F., Aller, J., (1997). Diachronous Variscan tectonothermal activity  
1006 in the NW Iberian Massif: Evidence from  $^{40}\text{Ar}/^{39}\text{Ar}$  dating of regional fabrics.  
1007 *Tectonophysics*, 277, 307-337. [https://doi.org/10.1016/S0040-1951\(97\)00035-8](https://doi.org/10.1016/S0040-1951(97)00035-8)  
1008  
1009 Delgado Quesada, M., (1971). Esquema geológico de la Hoja núm. 878 de Azuaga,  
1010 Badajoz. *Boletín Geológico y Minero* 82, 277-286.  
1011  
1012 Delgado Quesada, M.; Liñán, E.; Pascual, E.; Pérez-Lorente, F., (1977). Criterios para la  
1013 diferenciación de Dominios en Sierra Morena Central. *Studia geologica salmanticensia.*,  
1014 12, 75-90.  
1015  
1016 DePaolo, D.J., (1981). Neodymium isotopes in the Colorado Front Range and crustal-  
1017 mantle evolution in the Proterozoic. *Nature* 291, 193–196.

1018 <https://doi.org/10.1038/291193a0>

1019

1020 DePaolo, D.J., (1983). The mean life of continents: Estimates of continent recycling rates

1021 from Nd and Hf isotopic data and implications for mantle structure. *Geophysical*

1022 *Research Letters* 10: 705-708. doi:10.1029/GL010i008p00705

1023

1024 Díaz García, F., Sánchez Martínez, S., Castiñeiras, P., Fuenlabrada, J.M., Arenas, R.,

1025 (2010). A peri-Gondwanan arc in NW Iberia. II: assessment of the intra-arc

1026 tectonothermal evolution through U–Pb SHRIMP dating of mafic dykes. *Gondwana*

1027 *Research* 17, 352–362. <https://doi.org/10.1016/j.gr.2009.09.010>

1028

1029 Díez Fernández, R., Arenas, R., (2015). The Late Devonian Variscan suture of the Iberian

1030 Massif: a correlation of high-pressure belts in NW and SW Iberia. *Tectonophysics* 654,

1031 96–100. <https://doi.org/10.1016/j.tecto.2015.05.001>

1032

1033 Díez Fernández, R., Martínez Catalán, J.R., Gerdes, A., Abati, J., Arenas, R., Fernández-

1034 Suárez, J., (2010). U–Pb ages of detrital zircons from the Basal allochthonous units of

1035 NW Iberia: provenance and paleoposition on the northern margin of Gondwana during

1036 the Neoproterozoic and Paleozoic. *Gondwana Research* 18, 385–399.

1037 <https://doi.org/10.1016/j.gr.2009.12.006>

1038

1039 Díez Fernández, R., Arenas, R., Francisco Pereira, M., Sánchez Martínez, S., Albert

1040 Roper, R., Martín Parra, L.M., Rubio Pascual, F.J., Matas, J., (2016). Tectonic evolution

1041 of Variscan Iberia: Gondwana–Laurussia collision revisited. *Earth-Science Reviews* 162,

1042 269–292. <https://doi.org/10.1016/j.earscirev.2016.08.002>

1043

1044 Díez Fernández, R., Fuenlabrada, J. M., Chichorro, M., Pereira, M. F., Sánchez Martínez,  
1045 S., Silva, J. B., Arenas, R., (2017). Geochemistry and tectonostratigraphy of the basal  
1046 allochthonous units of SW Iberia (Évora Massif, Portugal): Keys to the reconstruction of  
1047 pre-Pangean paleogeography in southern Europe. *Lithos*, 268-271, 285–301.  
1048 <https://doi.org/10.1016/j.lithos.2016.10.031>

1049

1050 Díez Fernández, R., Jiménez-Díaz, A., Arenas, R., Pereira, M. F., Fernández-Suárez, J.,  
1051 (2019). Ediacaran obduction of a fore-arc ophiolite in SW Iberia: A turning point in the  
1052 evolving geodynamic setting of peri-Gondwana. *Tectonics*, 38, 95–119.  
1053 <https://doi.org/10.1029/2018TC005224>

1054

1055 Drost, K., Gerdes, A., Jeffries, T., Linnemann, U., Storey, C., (2011). Provenance of  
1056 Neoproterozoic and early Paleozoic siliciclastic rocks of the Teplá-Barrandian unit  
1057 (Bohemian Massif): evidence from U–Pb detrital zircon ages. *Gondwana Research* 19,  
1058 213–231. <https://doi.org/10.1016/j.gr.2010.05.003>

1059

1060 Eguíluz, L., (1987). Petrogénesis de rocas ígneas y metamórficas en el Antiforme  
1061 Burguillos-Monesterio, Macizo Ibérico Meridional, (PhD thesis) (694 pp.). Universidad  
1062 del País Vasco.

1063

1064 Eguíluz, L., Gil Ibarra, J. I., Abalos, B., Apraiz, A., (2000). Superposed Hercynian  
1065 and Cadomian orogenic cycles in the Ossa-Morena zone and related areas of the Iberian  
1066 Massif. *Geological Society of America Bulletin*, 112(9), 1398–1413.  
1067 [https://doi.org/10.1130/0016-7606\(2000\)112<1398:SHACOC>2.0.CO;2](https://doi.org/10.1130/0016-7606(2000)112<1398:SHACOC>2.0.CO;2)

1068

1069 Farias, P., Gallastegui, G., González-Lodeiro, F., Marquínez, J., Martín Parra, L.M.,  
1070 Martínez Catalán, J.R., Pablo Maciá, J.G. de, Rodríguez Fernández, L.R., (1987).  
1071 Aportaciones al conocimiento de la litoestratigrafía y estructura de Galicia central 1.  
1072 Memórias da Faculdade de Ciências, Universidade do Porto, pp. 411–431.

1073

1074 Fedo, C.M., Nesbitt, H.W., Young, G.M., (1995). Unravelling the effects of potassium  
1075 metasomatism in sedimentary rocks and paleosols, with implications for paleoweathering  
1076 conditions and provenance. *Geology* 23, 921–924.

1077 [https://doi.org/10.1130/0091-7613\(1995\)023<0921:UTEOPM>2.3.CO;2](https://doi.org/10.1130/0091-7613(1995)023<0921:UTEOPM>2.3.CO;2)

1078

1079 Fernández-Suárez, J., Gutiérrez-Alonso, G., Jenner, G. A., Tubrett, M. N., (2000). New  
1080 ideas on the Proterozoic-Early Paleozoic evolution of NW Iberia: Insights from U-Pb  
1081 detrital zircon ages. *Precambrian Research* 102, 185–206.

1082 [https://doi.org/10.1016/S0301-9268\(00\)00065-6](https://doi.org/10.1016/S0301-9268(00)00065-6)

1083

1084 Fernández-Suárez, J., Corfu, F., Arenas, R., Marcos, A., Martínez Catalán, J.R., Díaz  
1085 García, F., Abati, J., Fernández, F.J., (2002a). U-Pb evidence for a polyorogenic evolution  
1086 of the HP-HT units of the NW Iberian Massif. *Contributions to Mineralogy and Petrology*  
1087 143, 236–253. <https://doi.org/10.1007/s00410-001-0337-2>

1088

1089 Fernández-Suárez, J., Gutiérrez-Alonso, G., Jeffries, T. E. (2002b). The importance of  
1090 along-margin terrane transport in northern Gondwana: Insights from detrital zircon  
1091 parentage in Neoproterozoic rocks from Iberia and Brittany. *Earth and Planetary Science*  
1092 *Letters*, 204 (1-2), 75–88. [https://doi.org/10.1016/S0012-821X\(02\)00963-9](https://doi.org/10.1016/S0012-821X(02)00963-9)

1093

1094 Fernández-Suárez, J., Díaz García, F., Jeffries, T.E., Arenas, R., Abati, J., (2003).

1095 Constraints on the provenance of the uppermost allochthonous terrane of the NW Iberian

1096 Massif: inferences from detrital zircon U-Pb ages. *Terra Nova* 15, 138–144.

1097 <https://doi.org/10.1046/j.1365-3121.2003.00479.x>

1098

1099 Fernández-Suárez, J., Gutiérrez-Alonso, G., Pastor-Galán, D., Hofmann, M., Murphy,

1100 J.B., Linnemann, U., (2014). The Ediacaran–Early Cambrian detrital zircon record of

1101 NW Iberia: possible sources and paleogeographic constraints. *International Journal of*

1102 *Earth Sciences* 103 (5), 1335–1357. <https://doi.org/10.1007/s00531-013-0923-3>

1103

1104 Floyd, P.A., Leveridge, B.E., (1987). Tectonic environment of the Devonian Gramscatho

1105 Basin, South Cornwall: framework mode and geochemical evidence from turbiditic

1106 sandstones. *Journal of the Geological Society* 144 (4), 531–542.

1107 <https://doi.org/10.1144/gsjgs.144.4.0531>

1108

1109 Fralick, P.W., Kronberg, B.I., (1997). Geochemical discrimination of clastic sedimentary

1110 rock sources, *Sedimentary Geology* 113 (1–2), 111–124. [https://doi.org/10.1016/S0037-](https://doi.org/10.1016/S0037-0738(97)00049-3)

1111 [0738\(97\)00049-3](https://doi.org/10.1016/S0037-0738(97)00049-3)

1112

1113 Franke, W., (1989). Tectonostratigraphic units in the Variscan belt of central Europe. In:

1114 Dallmeyer, R.D. (Ed.), *Terranes in the Circum-Atlantic Paleozoic Orogens*, pp. 67–90

1115 *Geological Society of America Special Paper*. <https://doi.org/10.1130/SPE230-p67>

1116

1117 Fricke, W., (1941). Die Geologie des Grenzgebietes zwischen nordöstlicher Sierra Morena  
1118 und Extremadura. Phd Thesis. University of Berlin, Berlin, Germany, p. 91  
1119

1120 Fuenlabrada, J.M., Arenas, R., Sánchez Martínez, S., Díaz García, F., Castiñeiras, P.,  
1121 (2010). A peri-Gondwanan arc in NW Iberia I: isotopic and geochemical constraints on  
1122 the origin of the arc – a sedimentary approach. *Gondwana Research*. 17, 338–351.  
1123 <https://doi.org/10.1016/j.gr.2009.09.007>  
1124

1125 Fuenlabrada, J.M., Arenas, R., Díez Fernández, R., Sánchez Martínez, S., Abati, J., López  
1126 Carmona, A., (2012). Sm-Nd isotope geochemistry and tectonic setting of the  
1127 metasedimentary rocks from the basal allochthonous units of NW Iberia (Variscan suture,  
1128 Galicia). *Lithos* 148, 196–208. <https://doi.org/10.1016/j.lithos.2012.06.002>  
1129

1130 Fuenlabrada, J.M., Pieren, A.P., Díez Fernández, R., Sánchez Martínez, S., Arenas, R.,  
1131 (2016). Geochemistry of the Ediacaran-Early Cambrian transition in Central Iberia:  
1132 tectonic setting and isotopic sources. *Tectonophysics* 681, 15–30.  
1133 <https://doi.org/10.1016/j.tecto.2015.11.013>  
1134

1135 Fuenlabrada, J.M., Arenas, R., Sánchez Martínez, S., Díez Fernández, R., Pieren, A.P.,  
1136 Pereira, M.F., Chichorro, M., Silva, J.B., (2020). Geochemical and isotopic (Sm-Nd)  
1137 provenance of Ediacaran-Cambrian metasedimentary series from the Iberian Massif.  
1138 Paleoreconstruction of the North Gondwana margin. *Earth-Science Reviews* 201.  
1139 103079. <https://doi.org/10.1016/j.earscirev.2019.103079>  
1140

- 1141 Garcia, D., Coelho, J., Perrin, M., (1991). Fractionation between TiO<sub>2</sub> and Zr as a  
1142 measure of sorting within shale and sandstone series (Northern Portugal). *European*  
1143 *Journal of Mineralogy* 3 (2), 401-414. doi: 10.1127/ejm/3/2/0401  
1144
- 1145 Garrote, A., (1976). Asociaciones minerales del núcleo metamórfico de Sierra Albarrana  
1146 (prov. de Córdoba). Sierra Morena Central. *Memorias e Noticias, publ. Mus. Lab.*  
1147 *Mineral. Geol. Univ. Coímbra*, 82, pp. 17-39.  
1148
- 1149 Garrote, A., Ortega Huertas, M., Romero, J., (1980). Los yacimientos de pegmatitas de  
1150 Sierra Albarrana (Provincia de Córdoba, Sierra Morena). 1ª Reunión sobre la geología de  
1151 Ossa-Morena. *Temas Geológicos Mineros, IGME, Madrid*, 145-168.  
1152
- 1153 González del Tánago, J., Peinado, M., (1990). Contribución al estudio del metamorfismo  
1154 de Sierra Albarrana (Z.O.M., Córdoba, España). *Boletín Geológico y Minero* 101, 18-40.  
1155
- 1156 González del Tánago, J., Arenas, R., (1991). Anfibolitas granatíferas de Sierra Albarrana  
1157 (Córdoba). *Termobarometría e implicaciones para el desarrollo del metamorfismo*  
1158 *regional. Revista de la Sociedad Geológica de España* 4, 251–269.  
1159
- 1160 González del Tánago, J., (1995). El núcleo metamórfico de sierra albarrana y su campo  
1161 de pegmatitas graníticas asociado, macizo Ibérico, Córdoba, España. *Ediciós do Castro,*  
1162 *Sada, serie Nova Terra* 12 (511 pp).  
1163
- 1164 Gutiérrez-Marco, J. C., San José, M. A., Pieren, A. P. (1990): Central-Iberian Zone,  
1165 Autochthonous sequences: post-Cambrian Palaeozoic Stratigraphy. In: R. D. Dallmeyer,

1166 E. Martínez García (eds.) Pre-Mesozoic Geology of Iberia: 160-171, Springer-Verlag,  
1167 Berlin. [https://doi.org/10.1007/978-3-642-83980-1\\_14](https://doi.org/10.1007/978-3-642-83980-1_14)  
1168  
1169 Henderson, B.J., Collins, W.J., Murphy, J.B., Gutierrez-Alonso, G., Hand, M., (2016).  
1170 Gondwanan basement terranes of the Variscan–Appalachian orogen: Baltican, Saharan  
1171 and West African hafnium isotopic fingerprints in Avalonia, Iberia and the Armorican  
1172 Terranes, *Tectonophysics* 681, 278-304. <https://doi.org/10.1016/j.tecto.2015.11.020>  
1173  
1174 Herron, M.M., (1988). Geochemical classification of terrigenous sands and shales from  
1175 core or log data. *Journal of Sedimentary Research* 58, 820–829.  
1176 <https://doi.org/10.1306/212F8E77-2B24-11D7-8648000102C1865D>  
1177  
1178 Hiscott, R.N., (1984). Ophiolitic source rocks for Taconic-age flysch: Trace-element  
1179 evidence. *Geological Society of America Bulletin* 95, 1261-1267.  
1180 [https://doi.org/10.1130/0016-7606\(1984\)95<1261:OSRFTF>2.0.CO;2](https://doi.org/10.1130/0016-7606(1984)95<1261:OSRFTF>2.0.CO;2)  
1181  
1182 IGME, (2015). Mapa geológico de España y Portugal E: 1.1000.000. Instituto Geológico  
1183 y Minero de España, Madrid. Depósito Legal: M-35958-2014  
1184  
1185 Insúa M., Carvajal, A., Huerta, J., Matas, J., (1990). Memoria de la Hoja nº 900 (La  
1186 Cardenchoa). Mapa Geológico de España E. 1:50.000 (MAGNA), Segunda Serie,  
1187 Primera edición. IGME, 80 pp. Depósito legal: M-22390-2007.  
1188 ISBN: 978-84-7840-685-2  
1189



1190 Jacobsen, S.B., Wasserburg, G.J., (1980). Sm-Nd isotopic evolution of chondrites. Earth  
1191 and Planetary Science Letters, 50, 139-155.  
1192 [https://doi.org/10.1016/0012-821X\(80\)90125-9](https://doi.org/10.1016/0012-821X(80)90125-9)  
1193

1194 Jensen, S., Palacios, T., Eguíluz, L., (2004). Cambrian ichnofabrics from the Ossa Morena  
1195 and Central Iberian zones: preliminary results. Geo-temas 6(2), 291-293.  
1196

1197 Julivert, M., Fontboté, J.M., Ribeiro, A., Conde, L., (1972). Mapa Tectónico de la  
1198 Península Ibérica y Baleares E. 1:1.000.000. Instituto Geológico y Minero de España,  
1199 Madrid. Depósito Legal: M-21994-1972.  
1200

1201 Kroner, U., Romer, R.L., (2013). Two plates – Many subduction zones: The Variscan  
1202 orogeny reconsidered. Gondwana Research. 24, 298–329.  
1203 <https://doi.org/10.1016/j.gr.2013.03.001>  
1204

1205 Linnemann, U., Romer, R.L., (2002). The Cadomian Orogeny in Saxo-Thuringia,  
1206 Germany: geochemical and Nd–Sr–Pb isotopic characterization of marginal basins with  
1207 constraints to geotectonic setting and provenance. Tectonophysics 352, 33–64.  
1208 [https://doi.org/10.1016/S0040-1951\(02\)00188-9](https://doi.org/10.1016/S0040-1951(02)00188-9)  
1209

1210 Linnemann, U., Gerdes, A., Drost, K., Buschmann, B., (2007). The continuum between  
1211 Cadomian orogenesis and opening of the Rheic Ocean: constraints from LA-ICP-MS U-  
1212 Pb zircon dating and analysis of plate-tectonic setting (Saxo-Thuringian zone,  
1213 northeastern Bohemian Massif, Germany). In: Linnemann, U., Nance, R.D., Kraft, P.,  
1214 Zulauf, G. (Eds.), The evolution of the Rheic Ocean: From Avalonian–Cadomian Active

1215 Margin to Alleghenian–Variscan Collision. 423. pp. 61–96 Geological Society of  
1216 America Special Paper. Boulder Colorado. [https://doi.org/10.1130/2007.2423\(03\)](https://doi.org/10.1130/2007.2423(03))  
1217

1218 Linnemann, U., Pereira, F., Jeffries, T.E., Drost, K., Gerdes, A., (2008). The Cadomian  
1219 Orogeny and the opening of the Rheic Ocean: the diachrony of the geotectonic processes  
1220 constrained by LA-ICP-MS U–Pb zircon dating (Ossa-Morena and Saxo-Thuringian  
1221 zones, Iberian and Bohemian massifs). *Tectonophysics* 461(1-4), 21–43.  
1222 <https://doi.org/10.1016/j.tecto.2008.05.002>  
1223

1224 Linnemann, U., Gerdes, A., Hofmann, M., Marko, L., (2014). The Cadomian Orogen:  
1225 Neoproterozoic to Early Cambrian crustal growth and orogenic zoning along the  
1226 periphery of the West African Craton – Constraints from U-Pb zircon ages and Hf  
1227 isotopes (Schwarzburg Antiform, Germany). *Precambrian Research* 244, 236–278.  
1228 <https://doi.org/10.1016/j.precamres.2013.08.007>  
1229

1230 Liñán, E., (1978). Bioestratigrafía de la Sierra de Córdoba [PhD]: Universidad de  
1231 Granada, 212 p.  
1232

1233 Liñán, E., (1984). Los icnofósiles de la Formación Torreárboles (¿Precámbrico?-  
1234 Cámbrico Inferior) en los alrededores de Fuente de Cantos, Badajoz. Cuadernos do  
1235 Laboratorio Xeoloxico de Laxe, 8, 47–74.  
1236

1237 Liñán, E., Palacios, T., (1983). Aportaciones micropaleontológicas para el conocimiento  
1238 del límite Precámbrico-Cámbrico en la Sierra de. Córdoba, España. *Comunicações dos*  
1239 *Serviços Geológicos de Portugal*, 69, 227–234.

1240

1241 Liñán, E., Palacios, T., Perejón, A., (1984). Precambrian—Cambrian boundary and  
1242 correlation from southwestern and central part of Spain. *Geological Magazine*, 121(03),  
1243 221–228. <https://doi.org/10.1017/S0016756800028284>

1244

1245 Liñán, E., Quesada, C., (1990). Ossa-Morena Zone: 2. Stratigraphy. Rift phase, in  
1246 Dallmeyer, R. D., and Martínez García, E., eds., *Pre-Mesozoic Geology of Iberia*: Berlin,  
1247 Germany, Springer- Verlag, p. 259–266.

1248

1249 López Guijarro, R., (2006). Ambiente geodinámico y procedencia de las rocas  
1250 sedimentarias precámbricas de las zonas de Ossa Morena y Centroibérica a través del  
1251 análisis geoquímico. *Boletín Geológico y Minero*, 117 (Núm. Monográfico Especial):  
1252 499-505. ISSN: 0366-0176

1253

1254 López Guijarro, R., Armendariz, M., Quesada, C., Fernández-Suárez, J., Murphy, J.B.,  
1255 Pin, C., Bellido, F., (2008). Ediacaran–Palaeozoic tectonic evolution of the Ossa Morena  
1256 and Central Iberian zones (SW Iberia) as revealed by Sm–Nd isotope systematics.  
1257 *Tectonophysics* 461 (1-4), 202–214. <https://doi.org/10.1016/j.tecto.2008.06.006>

1258

1259 Lotze, F., (1945). Zur gliederung der varisziden der iberischen meseta. *Geotekt. Forsch.*  
1260 6, 78–92.

1261

1262 Lugmair, G.W, and Marti, K., (1978). Lunar initial  $^{143}\text{Nd}/^{144}\text{Nd}$  differential evolution of  
1263 the lunar crust and mantle. *Earth and Planetary Science Letters*, 39, 349-357.

1264 [https://doi.org/10.1016/0012-821X\(78\)90021-3](https://doi.org/10.1016/0012-821X(78)90021-3)

1265

1266 Marcos, A., Azor, A., González Lodeiro, F., Simancas, F., (1991). Early Phanerozoic  
1267 trace fossils from the Sierra Albarrana Quartzites (Ossa-Morena Zone, Southwest Spain),  
1268 *Scripta Geologica* 97, 47-53.

1269

1270 Martín Parra, L.M., González Lodeiro, F., Martínez Poyatos, D., Matas, J., (2006). The  
1271 Puente Génave-Castelo de Vide Shear Zone (southern Central Iberian Zone, Iberian  
1272 Massif): geometry, kinematics and regional implications. *Bulletin de la Société*  
1273 *Géologique de France* 177, 191–202. <https://doi.org/10.2113/gssgfbull.177.4.191>

1274

1275 Martínez Catalán, J.R., Arenas, R., Díaz García, F., Abati, J., (1997). Variscan  
1276 accretionary complex of northwest Iberia: terrane correlation and succession of  
1277 tectonothermal events. *Geology* 25, 1103–1106.  
1278 [https://doi.org/10.1130/0091-7613\(1997\)025<1103:VACONI>2.3.CO;2](https://doi.org/10.1130/0091-7613(1997)025<1103:VACONI>2.3.CO;2)

1279

1280 Martínez Catalán, J.R., Arenas, R., Díaz García, F., Gómez Barreiro, J., González Cuadra,  
1281 P., Abati, J., Castiñeiras, P., Fernández-Suárez, J., Sánchez Martínez, S., Andonaegui, P.,  
1282 González Clavijo, E., Díez Montes, A., Rubio Pascual, F.J., Valle Aguado, B., (2007).  
1283 Space and time in the tectonic evolution of the northwestern Iberian Massif. Implications  
1284 for the Variscan belt. In: Hatcher, R.D., Carlson, M.P., McBride, J.H., Martínez Catalán,  
1285 J.R. (Eds.), *4-D Framework of Continental Crust*, pp. 403–423 Geological Society of  
1286 America Memoir, Boulder, Colorado. [https://doi.org/10.1130/2007.1200\(21\)](https://doi.org/10.1130/2007.1200(21))

1287

1288 Martínez Catalán, J.R., Arenas, R., Abati, J., Sánchez Martínez, S., Díaz García, F.,  
1289 Fernández-Suárez, J., González Cuadra, P., Castiñeiras, P., Gómez Barreiro, J., Díez

1290 Montes, A., González Clavijo, E., Rubio Pascual, F.J., Andonaegui, P., Jeffries, T.E.,  
1291 Alcock, J.E., Díez Fernández, R., López Carmona, A., (2009). A rootless suture and the  
1292 loss of the roots of a mountain chain: The Variscan belt of NW Iberia. *Comptes Rendus*  
1293 *Geoscience* 341 (2-3), 114–126. <https://doi.org/10.1016/j.crte.2008.11.004>  
1294  
1295 Martínez Catalán, J.R., Collett, S., Schulmann, K., Aleksandrowski, P., Mazur, S., (2020).  
1296 Correlation of allochthonous terranes and major tectonostratigraphic domains between  
1297 NW Iberia and the Bohemian Massif, European Variscan belt. *International Journal of*  
1298 *Earth Sciences (Geol Rundsch)* 109, 1105–1131. [https://doi.org/10.1007/s00531-019-](https://doi.org/10.1007/s00531-019-01800-z)  
1299 [01800-z](https://doi.org/10.1007/s00531-019-01800-z)  
1300  
1301 Martínez Poyatos, D., (1997). Estructura del Borde Meridional de la Zona Centroibérica  
1302 y su Relación con el Contacto entre las Zonas Centroibérica y de Ossa-Morena. Tesis  
1303 Doct., Univ. Granada, 222 pp.  
1304  
1305 Matte, P., (1991). Accretionary history and crustal evolution of the Variscan belt in  
1306 Western Europe. *Tectonophysics* 196, 309–337. [https://doi.org/10.1016/0040-](https://doi.org/10.1016/0040-1951(91)90328-P)  
1307 [1951\(91\)90328-P](https://doi.org/10.1016/0040-1951(91)90328-P)  
1308  
1309 McLennan, S.M., (1989). Rare earth elements in sedimentary rocks: influence of  
1310 provenance and sedimentary processes. *Mineralogical Society of America, Review in*  
1311 *Mineralogy* 21, 169–200.  
1312  
1313 McLennan, S.M., Taylor, S.R., (1991). Sedimentary rocks and crustal evolution: tectonic  
1314 settings and secular trends. *Journal of Geology* 99, 1–21.

1315

1316 McLennan, S.M., Hemming, S., (1992). Samarium/neodymium elemental and isotopic  
1317 systematics in sedimentary rocks. *Geochimica et Cosmochimica Acta* 56 (3), 887–898.

1318 [https://doi.org/10.1016/0016-7037\(92\)90034-G](https://doi.org/10.1016/0016-7037(92)90034-G)

1319

1320 McLennan, S.M., Hemming, S.R., McDaniel, D.K., Hanson, G.N., (1993). Geochemical  
1321 approaches to sedimentation, provenance and tectonics. In: Johnssons, M.J., Basu, A.  
1322 (Eds.), processes controlling the composition of clastic sediments. *Geol. Soc. Am. Spec.*  
1323 *Pap.* 284, 21–40. <https://doi.org/10.1130/SPE284-p21>

1324

1325 McLennan, S.M., Taylor, S.R., Hemming, S.R., (2006). Composition, differentiation, and  
1326 evolution of continental crust: constrains from sedimentary rocks and heat flow. In:  
1327 Brown M, Rushmer T (eds) *Evolution and differentiation of the continental crust*.  
1328 Cambridge University Press, Cambridge, 92–134.

1329

1330 Mielke, J.E., (1979). Composition of the Earth's crust and distribution of the elements.  
1331 In: F. R. Siegel (Ed.), *Review of research on modern problems in geochemistry*.  
1332 International Association for Geochemistry and Cosmochemistry. *Earth Science Series*  
1333 *No. 16*. UNESCO Report SC/GEO/544/3, Paris, 13-37.

1334

1335 Moita, P., Munhá, J., Fonseca, P.E., Pedro, J., Tassinari, C.C.G., Araújo, A., Palacios, T.,  
1336 (2005). Phase equilibria and geochronology of Ossa-Morena eclogites, XIV Semana de  
1337 Geoquímica, VIII Congresso de Geoquímica dos Países de Língua Portuguesa, pp. 463-  
1338 466.

1339

1340 Morag, N., Avigad, D., Gerdes, A., Belousova, E., Harlavan, Y., (2011). Detrital zircon  
1341 Hf isotopic composition indicates long-distance transport of North Gondwana Cambrian–  
1342 Ordovician sandstones. *Geology* 39, 955–958. <https://doi.org/10.1130/G32184.1>  
1343  
1344 Murphy, J.B., Nance, R.D., (1989). Model for the evolution of the Avalonian–Cadomian  
1345 belt. *Geology* 17 (8), 735–738.  
1346 [https://doi.org/10.1130/0091-7613\(1989\)017<0735:MFTEOT>2.3.CO;2](https://doi.org/10.1130/0091-7613(1989)017<0735:MFTEOT>2.3.CO;2)  
1347  
1348 Nägler, T.F., Schiller, H.J., Gebauer, D., (1995). Evolution of the Western European  
1349 continental crust: implications from Nd and Pb isotopes in Iberian sediments. *Chemical*  
1350 *Geology* 121, 345–357. [https://doi.org/10.1016/0009-2541\(94\)00129-V](https://doi.org/10.1016/0009-2541(94)00129-V)  
1351  
1352 Nakamura, N., (1974). Determination of REE, Ba, Fe, Mg, Na and K in carbonaceous  
1353 and ordinary chondrites. *Geochimica et Cosmochimica Acta* 38, 757–775.  
1354 [https://doi.org/10.1016/0016-7037\(74\)90149-5](https://doi.org/10.1016/0016-7037(74)90149-5)  
1355  
1356 Nance, R.D., Gutiérrez-Alonso, G., Keppi, J.D., Linnemann, U., Murphy, J.B., Quesada,  
1357 C., Strachan, R.A., Woodcock, N.H., (2010). Evolution of the Rheic Ocean. *Gondwana*  
1358 *Research* 17 (2-3), 194–222. <https://doi.org/10.1016/j.gr.2009.08.001>  
1359  
1360 Nesbitt, H.W., Young, G.M., (1982). Early Proterozoic climates and plate motions  
1361 inferred from major element chemistry of lutites. *Nature* 299, 715–717.  
1362 <https://doi.org/10.1038/299715a0>  
1363

1364 O'Nions, R.K., Carter, S.R., Evensen, N.M., Hamilton, P.J., (1979). Geochemical and  
1365 cosmochemical applications of Nd isotope analysis. *Annual Review of Earth and*  
1366 *Planetary Sciences* 7, 11–38.

1367

1368 Ordóñez-Casado, B., Gebauer, D., Eguiluz, L., (1998). SHRIMP age-constraints for the  
1369 calc-alkaline volcanism in the Olivenza-Monesterio Antiform (Ossa-Morena, SW Spain).  
1370 *Mineralogical Magazine*, 62A (2), 1112–1113. [10.1180/minmag.1998.62A.2.248](https://doi.org/10.1180/minmag.1998.62A.2.248)

1371

1372 Ordoñez Casado, B., Gebauer, D., Eguíluz, L., (2009). Zircon ion-probe dating the  
1373 maximum age of deposition of the Montemolín succession (Lower Serie Negra) in the  
1374 Ossa Morena Zone, Spain. *Macla*, 11, 137–138.

1375

1376 Orejana, D., Merino Martínez, E., Villaseca, C., Andersen, T., (2015). Ediacaran–  
1377 Cambrian paleogeography and geodynamic setting of the Central Iberian Zone:  
1378 constraints from coupled U–Pb–Hf isotopes of detrital zircons. *Precambrian Research*  
1379 261, 234–251. <https://doi.org/10.1016/j.precamres.2015.02.009>

1380

1381 Pastor-Galán, D., Gutiérrez-Alonso, G., Fernández-Suárez, J., Murphy, J.B., Nieto, F.,  
1382 (2013). Tectonic evolution of NW Iberia during the Paleozoic inferred from the  
1383 geochemical record of detrital rocks in the Cantabrian Zone. *Lithos* 182–183, 211–228.  
1384 <https://doi.org/10.1016/j.lithos.2013.09.007>

1385

1386 Pereira, M. F., Chichorro, M., Linnemann, U., Eguiluz, L., Silva, J. B., (2006). Inherited  
1387 arc signature in Ediacaran and Early Cambrian basins of the Ossa-Morena Zone (Iberian



1388 Massif, Portugal): Paleogeographic link with European and North African Cadomian  
1389 correlatives. *Precambrian Research* 144 (3-4), 297–315.  
1390 <https://doi.org/10.1016/j.precamres.2005.11.011>  
1391  
1392 Pereira, M.F., Chichorro, M., Williams, I.S., Silva, J.B., (2008). Zircon U–Pb  
1393 geochronology of paragneisses and biotite granites from the SW Iberian Massif  
1394 (Portugal): evidence for a paleogeographic link between the Ossa-Morena Ediacaran  
1395 basins and the West African craton. In: Liégeois, J.P., Nasser, E. (Eds.), *The boundaries*  
1396 *of the West African Craton: Geological Society of London Special Publication*, 297, pp.  
1397 385–408. <http://dx.doi.org/10.1144/SP297.18>  
1398  
1399 Pereira, M.F., Linnemann, U., Hofmann, M., Chichorro, M., Solá, A.R., Medina, J., Silva,  
1400 J.B., (2012a). The provenance of Late Ediacaran and Early Ordovician siliciclastic rocks  
1401 in the Southwest Central Iberian Zone: constraints from detrital zircon data on northern  
1402 Gondwana margin evolution during late Neoproterozoic. *Precambrian Research* 192–195,  
1403 166–189. <https://doi.org/10.1016/j.precamres.2011.10.019>  
1404  
1405 Pereira, M.F., Solá, A.R., Chichorro, M., Lopes, L., Gerdes, A., Silva, J.B., (2012b).  
1406 North Gondwana assembly, break-up and paleogeography: U–Pb isotope evidence from  
1407 detrital and igneous zircons of Ediacaran and Cambrian rocks of SW Iberia. *Gondwana*  
1408 *Research* 22 (3-4), 866–881. <https://doi.org/10.1016/j.gr.2012.02.010>  
1409  
1410 Pereira, M.F., (2015a). Potential sources of Ediacaran strata of Iberia: a review.  
1411 *Geodinamica Acta* 27 (1), 1-14, DOI: 10.1080/09853111.2014.957505  
1412

1413 Pereira, M.F., El Houicha, M., Chichorro, M., Armstrong, R., Jouhari, A., El Attari, A.,  
1414 Ennih, N., Silva, J.B., (2015b). Evidence of a Paleoproterozoic basement in the Moroccan  
1415 Variscan Belt (Rehamna Massif, Western Meseta), *Precambrian Research* 268, 61-73.  
1416 <https://doi.org/10.1016/j.precamres.2015.07.010>.  
1417  
1418 Pereira, M.F., Gama, C., Dias da Silva, I., Fuenlabrada, J.M., Brandão Silva, J., Medina,  
1419 J., (2020). Isotope geochemistry evidence for Laurussian-type sources of South-  
1420 Portuguese Zone Carboniferous turbidites (Variscan orogeny) Geological Society,  
1421 London, Special Publications, 503. <https://doi.org/10.1144/SP503-2019-163>  
1422  
1423 Pérez Estaún, A., Bea, F., Marcos, A., Martínez Catalán, J.R., Martínez Poyatos, D.,  
1424 Arenas, R., Díaz García, F., Azor, A., Simancas, F., González Lodeiro, F., (2004). La  
1425 cordillera varisca europea: el Macizo ibérico En: *Geología de España* (J.A. Vera, Ed.),  
1426 SGE-IGME, Madrid: 21-25.  
1427  
1428 Pieren Pidal, A.P., (2000). Las sucesiones anteordovícicas de la región oriental de la  
1429 provincial de Badajoz y área contigua de la de Ciudad Real. Thesis Universidad  
1430 Complutense Madrid, Ph. D (379 pp.).  
1431  
1432 Quesada, C., (1990). Precambrian successions in SW Iberia: their relationships to  
1433 Cadomian orogenic events. In: D'Lemos, R.S., Strachan, R.A., Topley, C.G. (Eds.), *The*  
1434 *Cadomian Orogeny*. Geological Society London, Special Publication, vol. 51, 353–362.  
1435 <http://dx.doi.org/10.1144/GSL.SP.1990.051.01.23>  
1436

1437 Quesada, C., Apalategui, O., Eguiluz, L., Liñán, E., Palacios, T., (1990), Ossa-Morena  
1438 Zone: Precambrian, in Dallmeyer, R. D., and Martínez-García, E., eds., Pre-mesozoic  
1439 geology of Iberia: Berlin, Springer, p. 250–258.  
1440  
1441 Ribeiro, A., Munhá, J., Dias, R., Mateus, A., Pereira, E., Ribeiro, L., Fonseca, P., Araújo,  
1442 A., Oliveira, T., Romão, J., Chaminé, H., Coke, C., Pedro, J., (2007). Geodynamic  
1443 evolution of the SW Europe Variscides. *Tectonics* 26, TC6009.  
1444 <https://doi.org/10.1029/2006TC002058>  
1445  
1446 Ries, A.C., Shackleton, R.M., (1971). Catazonal complexes of north-west Spain and north  
1447 Portugal, remnants of a Hercynian thrust plate. *Nature Physical Science* 234, 65–68.  
1448 <https://doi.org/10.1038/physci234065a0>  
1449  
1450 Robardet, M., (1976): L'originalité du segment hercynien sudibérique au Paléozoïque  
1451 inférieur: Ordovicien, Silurien et Dévonien dans le nord de la province de Séville  
1452 (Espagne). *Comptes Rendus de l'Académie des Sciences, Paris*, 283, série D: 999-1002.  
1453  
1454 Rodríguez Alonso, M.D., Díez Balda, M.A., Perejón, A., Pieren, A., Liñán, E., López  
1455 Díaz, F., Moreno, F., Gámez Vintaned, J.A., González Lodeiro, F., Martínez Poyatos, D.,  
1456 Vegas, R., (2004a). Dominio del Complejo esquisto-grauváquico. *Estratigrafía. La*  
1457 *secuencia litoestratigráfica del Neoproterozoico–Cámbrico inferior*. In: Vera, J.A. (Ed.),  
1458 *Geología de España. Sociedad Geológica de España – Instituto Geológico y Minero de*  
1459 *España, Madrid*, pp. 78–81.  
1460

1461 Rodríguez Alonso, M.D., Peinado, M., López-Plaza, M., Franco, P., Carnicero, A.,  
1462 Gonzalo, J.C., (2004b). Neoproterozoic–Cambrian synsedimentary magmatism in the  
1463 Central Iberian Zone (Spain): geology, petrology and geodynamic significance.  
1464 International Journal of Earth Sciences 93, 897–920. <https://doi.org/10.1007/s00531-004->  
1465 0425-4  
1466  
1467 Rojo-Pérez, E., Arenas, R., Fuenlabrada, J.M., Sánchez Martínez, S., Martín Parra, L.M.,  
1468 Matas, J., Pieren, A.P., Díez Fernández, R., (2019). Contrasting isotopic sources (Sm-Nd)  
1469 of Late Ediacaran series in the Iberian Massif: implications for the Central Iberian – Ossa  
1470 Morena boundary. Precambrian Research 324, 194–207.  
1471 <https://doi.org/10.1016/j.precamres.2019.01.021>  
1472  
1473 Rojo-Pérez, E., Fuenlabrada, J.M., Linnemann, U., Arenas, R., Sánchez Martínez, S.,  
1474 Díez Fernández, R., Martín Parra, L.M., Matas, J., Andonaegui, P., Fernández-Suárez, J.,  
1475 (submitted). Geochemistry and Sm-Nd isotopic sources of Late Ediacaran siliciclastic  
1476 series in the Ossa-Morena Complex: Iberian-Bohemian correlations. International Journal  
1477 of Earth Sciences.  
1478  
1479 Rubio Pascual, F.J., Matas, J., Martín Parra, L.M., (2013). High-pressure metamorphism  
1480 in the Early Variscan subduction complex of the SW Iberian Massif. Tectonophysics 592,  
1481 187–199. <https://doi.org/10.1016/j.tecto.2013.02.022>  
1482  
1483 San José, M.A., Pieren, A.P., García Hidalgo, F.J., Vilas, L., Herranz, P., Peláez, J.R.,  
1484 Perejón, A., (1990). Central Iberian Zone: ante-Ordovician stratigraphy. In: Dallmeyer,

1485 R.D., Martínez García, E. (Eds.), Pre-Mesozoic Geology of Iberia. Springer, Berlin  
1486 Heidelberg New York, pp. 147–159.  
1487  
1488 Sánchez Carretero, R., Carracedo, M., Eguíluz, L., Apalategui, O., (1989). El  
1489 magmatismo calcoalcalino del Precámbrico terminal en la Zona de Ossa-Morena (Macizo  
1490 Ibérico). *Revista de la Sociedad Geológica de España* 2, 7-21.  
1491  
1492 Sánchez Martínez, S., Arenas, R., Albert, R., Gerdes, A., Fernández-Suárez, J., (2020)  
1493 Updated geochronology and isotope geochemistry of the Vila de Cruces Ophiolite: A case  
1494 study of a peri-Gondwanan back-arc ophiolite. *Geological Society, London, Special  
1495 Publications*, 503. <https://doi.org/10.1144/SP503-2020-8>  
1496  
1497 Sánchez García, T., Quesada, C., Bellido, F., Dunning, G.R., González del Tánago, J.,  
1498 (2008). Two-step magma flooding of the upper crust during rifting: the Early Paleozoic  
1499 of the Ossa Morena Zone (SW Iberia). *Tectonophysics* 461, 72–90.  
1500 <https://doi.org/10.1016/j.tecto.2008.03.006>  
1501  
1502 Sánchez-García, T., Pereira, M.F., Bellido, F., Chichorro, M., Silva, J.B., Valverde-  
1503 Vaquero, P., Pin, Ch., Solá, A.R., (2014). Early Cambrian granitoids of North Gondwana  
1504 margin in the transition from a convergent setting to intra-continental rifting (Ossa-  
1505 Morena Zone, SW Iberia). *International Journal of Earth Sciences (Geol Rundsch)* 103,  
1506 1203–1218. <https://doi.org/10.1007/s00531-013-0939-8>  
1507  
1508 Sánchez-García, T., Chichorro, M., Solá, A.R., Álvaro, J.J., Díez-Montes, A., Bellido, F.,  
1509 Ribeiro, M.L., Quesada, C., Lopes, J.C., Dias da Silva, Í., González-Clavijo, E., Gómez

1510 Barreiro, J., López-Carmona, A., (2019). The Cambrian-Early Ordovician Rift Stage in  
1511 the Gondwanan Units of the Iberian Massif. In: Quesada C., Oliveira J. (eds) The Geology  
1512 of Iberia: A Geodynamic Approach. Regional Geology Reviews. Springer, Cham.  
1513 [https://doi.org/10.1007/978-3-030-10519-8\\_2](https://doi.org/10.1007/978-3-030-10519-8_2)  
1514

1515 Schäfer, H.-J., Gebauer, D., Nægler, T. F., Eguiluz, L., (1993). Conventional and ion-  
1516 microprobe U-Pb dating of detrital zircons of the Tentudía Group (Serie Negra, SW  
1517 Spain): Implications for zircon systematics, stratigraphy, tectonics and the  
1518 Precambrian/Cambrian boundary. *Contributions to Mineralogy and Petrology*, 113(3),  
1519 289–299. <https://doi.org/10.1007/BF00286922>  
1520

1521 Simancas, J.F., Galindo-Zaldívar, J. Azor, A., (2000). Three-dimensional shape and  
1522 emplacement of the Cardenchocha deformed pluton (Variscan Orogen, southwestern  
1523 Iberian Massif). *Journal of Structural Geology* 22(4), 489–503.  
1524

1525 Simancas, J.F., Azor, A., Martínez-Poyatos, D., Tahiri, A., El Hadi, H., González-  
1526 Lodeiro, F., Pérez-Estaún, A., Carbonell, R., (2009). Tectonic relationships of Southwest  
1527 Iberia with the allochthons of Northwest Iberia and the Moroccan Variscides. *Comptes*  
1528 *Rendus Geoscience* 341, 103–113. <https://doi.org/10.1016/j.crte.2008.11.003>  
1529

1530 Stampfli, G.M., von Raumer, J., Borel, G.D., (2002). Paleozoic evolution of pre-Variscan  
1531 terranes: from Gondwana to the Variscan collision. In: Martínez Catalán, J.R., Hatcher  
1532 Jr., R.D., Arenas, R., Díaz García, F. (Eds.), *Variscan-Appalachian Dynamics: The*  
1533 *Building of the Late Paleozoic Basement*. Geological Society of America Special Paper  
1534 vol. 364, pp. 263–280. <https://doi.org/10.1130/0-8137-2364-7.263>

1535

1536 Stampfli, G.M., Hochard, C., Vérard, C., Wilhem, C., von Raumer, J., (2013). The  
1537 formation of Pangea. *Tectonophysics* 593, 1–19.

1538 <https://doi.org/10.1016/j.tecto.2013.02.037>

1539

1540 Stephan, T., Kroner, U., Romer, R.L., Rösel, D., (2019a). From a bipartite Gondwanan  
1541 shelf to an arcuate Variscan belt: the early Paleozoic evolution of northern Peri-  
1542 Gondwana. *Earth-Science Reviews* 192, 491–512.

1543 <https://doi.org/10.1016/j.earscirev.2019.03.012>

1544

1545 Stephan, T., Kroner, U., Romer, R.L., (2019b). The pre-orogenic detrital zircon record of  
1546 the Peri-Gondwanan crust. *Geological Magazine* 156 (2), 281–307.

1547 <https://doi.org/10.1017/S0016756818000031>

1548

1549 Stern, Robert J., (2002). Crustal evolution in the East African Orogen: a neodymium  
1550 isotopic perspective. *Journal of African Earth Sciences* 34 (3–4), 109–117.

1551 [https://doi.org/10.1016/S0899-5362\(02\)00012-X](https://doi.org/10.1016/S0899-5362(02)00012-X)

1552

1553 Talavera, C., Montero, P., Martínez Poyatos, D., Williams, I.S., (2012). Ediacaran to  
1554 Lower Ordovician age for rocks ascribed to the Schist–Graywacke Complex (Iberian  
1555 Massif, Spain): evidence from detrital zircon SHRIMP U-Pb geochronology. *Gondwana*

1556 *Research* 22, 928–942. <https://doi.org/10.1016/j.gr.2012.03.008>

1557

1558 Talavera, C., Montero, P., Bea, F., González Lodeiro, F., Whitehouse, M., (2013). U-Pb  
1559 Zircon geochronology of the Cambro-Ordovician metagranites and metavolcanic rocks  
1560 of central and NW Iberia. *International Journal of Earth Sciences* 102, 1–23.  
1561 <https://doi.org/10.1007/s00531-012-0788-x>  
1562  
1563 Tanaka, T., Togashi, S., Kamioka, H., Amakawa, H., Kagami, H., Hamamoto, T., Yuhara,  
1564 M., Orihashi, Y., Yoneda, S., Shimizu, H., Kunimaru, T., Takahashi, K., Yanagi, T.,  
1565 Nakano, T., Fujimaki, H., Shinjo, R., Asahara, Y., Tanimizu, M., Dragusanu, C., (2000).  
1566 JNdi-1: a neodymium isotopic reference in consistency with La Jolla neodymium.  
1567 *Chemical Geology* 168, 279–281 [https://doi.org/10.1016/S0009-2541\(00\)00198-4](https://doi.org/10.1016/S0009-2541(00)00198-4)  
1568  
1569 Taylor, S.R., McLennan, S.M., (1985). *The Continental Crust: Its Composition and*  
1570 *Evolution*. Blackwell, Oxford, p. 312. ISBN-13: 978–0632011483  
1571  
1572 Taylor, S.R., McLennan, S.M., (1988). The significance of the rare earths in geochemistry  
1573 and cosmochemistry, *Handbook on the Physics and Chemistry of Rare Earths*, Elsevier,  
1574 Volume 11, 485-578. ISSN 0168-1273, ISBN 9780444870803,  
1575 [https://doi.org/10.1016/S0168-1273\(88\)11011-8](https://doi.org/10.1016/S0168-1273(88)11011-8).  
1576  
1577 Ugidos, J.M., Billström, K., Valladares, M.I., Barba, P., (2003a). Geochemistry of the  
1578 Upper Neoproterozoic and Lower Cambrian siliciclastic rocks and U-Pb dating on detrital  
1579 zircons in the Central Iberian Zone, Spain. *International Journal of Earth Sciences* 92,  
1580 661–676.  
1581 <https://doi.org/10.1007/s00531-003-0355-6>  
1582



1583 Ugidos, J.M., Valladares, M.I., Barba, P., Ellam, R.M., (2003b). The Upper  
1584 Neoproterozoic–Lower Cambrian of the Central Iberian Zone, Spain: chemical and  
1585 isotopic (Sm-Nd) evidence that the sedimentary succession records an inverted  
1586 stratigraphy of its source. *Geochimica et Cosmochimica Acta* 67, 2615–2629.  
1587 [https://doi.org/10.1016/S0016-7037\(03\)00027-9](https://doi.org/10.1016/S0016-7037(03)00027-9)  
1588  
1589 Valladares, M.I., Barba, P., Ugidos, J.M., Colmenero, J.R., Armenteros, I., (2000). Upper  
1590 Neoproterozoic–Lower Cambrian sedimentary successions in the Central Iberian Zone  
1591 (Spain): sequence stratigraphy, petrology and chemostratigraphy. Implications for other  
1592 European zones. *International Journal of Earth Sciences* 89, 2–20.  
1593  
1594 Valladares, M.I., Ugidos, J.M., Barba, P., Colmenero, J.R., (2002). Contrasting  
1595 geochemical features of the Central Iberian Zone shales (Iberian Massif, Spain):  
1596 implications for the evolution of Neoproterozoic–Lower Cambrian sediments and their  
1597 sources in other Peri-Gondwanan areas. *Tectonophysics* 352, 121–132.  
1598 [https://doi.org/10.1016/S0040-1951\(02\)00192-0](https://doi.org/10.1016/S0040-1951(02)00192-0)  
1599  
1600 Villaseca, C., Merino, E., Oyarzun, R., Orejana, D., Pérez-Soba, C., Chicharro, E.,  
1601 (2014). Contrasting chemical and isotopic signatures from Neoproterozoic  
1602 metasedimentary rocks in the Central Iberian Zone (Spain) of pre-Variscan Europe:  
1603 implications for terrane analysis and Early Ordovician magmatic belts. *Precambrian*  
1604 *Research* 245, 131–145. <https://doi.org/10.1016/j.precamres.2014.02.006>  
1605

1606 von Raumer, J.F., Stampfli, G.M., Borel, G.D., Bussy, F., (2002). The organization of  
1607 pre-Variscan basement areas at the Gondwana margin. *International Journal of Earth*  
1608 *Sciences* 91, 35–52. <https://doi.org/10.1007/s005310100200>  
1609  
1610 von Raumer, J.F., Stampfli, G.A., Bussy, F., (2003). Gondwana-derived microcontinents  
1611 – the constituents of the Variscan and Alpine collisional orogens. *Tectonophysics* 365,  
1612 7–22. [https://doi.org/10.1016/S0040-1951\(03\)00015-5](https://doi.org/10.1016/S0040-1951(03)00015-5)  
1613  
1614 Whitney, D.L., Evans, B.W., (2010). Abbreviations for names of rock forming minerals.  
1615 *American Mineralogist* 95, 185-187. <https://doi.org/10.2138/am.2010.3371>  
1616  
1617 Winchester, J.A., Floyd, P.A., (1977). Geochemical discrimination of different magma  
1618 series and their differentiation products using immobile elements. *Chemical Geology*  
1619 20:325–343. [https://doi.org/10.1016/0009-2541\(77\)90057-2](https://doi.org/10.1016/0009-2541(77)90057-2)  
1620  
1621 Winchester, J.A., Max, M.D., (1989). Tectonic setting discrimination in clastic  
1622 sequences: an example from the late proterozoic Erris Group, NW Ireland. *Precambrian*  
1623 *Research* 45 (1-3), 191–201. [https://doi.org/10.1016/0301-9268\(89\)90039-9](https://doi.org/10.1016/0301-9268(89)90039-9)  
1624  
1625 Winchester, J.A., Pharaoh, T.C., Verniers, J., (2002). Palaeozoic amalgamation of Central  
1626 Europe: an introduction and synthesis of new results from recent geological and  
1627 geophysical investigations. In: Winchester, J.A., Pharaoh, T.C., Verniers, J. (Eds.),  
1628 *Palaeozoic Amalgamation of Central Europe*. Geological Society, London, Special  
1629 *Publications* vol. 201, pp. 1–18. <http://dx.doi.org/10.1144/GSL.SP.2002.201.01.01>  
1630

1631 Zhao, J.X., McCulloch, M.T., Bennett, V.C., (1992). Sm–Nd and U–Pb zircon isotopic  
1632 constraints on the provenance of sediments from the Amadeus Basin, central Australia:  
1633 evidence for REE fractionation. *Geochimica et Cosmochimica Acta* 56 (3), 921–940.  
1634 [https://doi.org/10.1016/0016-7037\(92\)90037-J](https://doi.org/10.1016/0016-7037(92)90037-J)

1635

## 1636 **Figure Captions**

1637

1638 **Figure 1.** (A) Zonation of the Variscan Orogen (Díez Fernández and Arenas, 2015;  
1639 Arenas et al., 2016b). (B) Geological map of the Iberian Massif showing the distribution  
1640 of autochthonous and allochthonous terranes in NW and SW Iberia (Díez Fernández and  
1641 Arenas, 2015). Location of the geological map presented in Figure 2 is shown.  
1642 Abbreviations: AF - Azuaga Fault; BAO - Beja–Acebuches Ophiolite; CA - Carvalhal  
1643 Amphibolites; CF – Canaleja Fault; CMU - Cubito–Moura Unit; CO - Calzadilla  
1644 Ophiolite; CU - Central Unit; ET - Espina Thrust; HF - Hornachos Fault; IOMZO -  
1645 Internal Ossa-Morena Zone Ophiolites; LLF - Llanos Fault; MLF - Malpica–Lamego  
1646 Fault; OF - Onza Fault; OVD - Obejo–Valsequillo Domain; PG–CVD - Puente Génave–  
1647 Castelo de Vide Detachment; PRF- Palas de Rei Fault; PTF - Porto–Tomar Fault; RF -  
1648 Riás Fault; VF - Viveiro Fault.

1649

1650 **Figure 2.** Geological map of the Central Iberian Zone – Ossa-Morena Complex boundary  
1651 (Rojo-Pérez et al., 2019; Based on the 1:1.000.000 geological map of Spain and Portugal,  
1652 IGME, 2015). Abbreviations: AF, Azuaga Fault; PG-CVD, Puente Génave – Castelo de  
1653 Vide Detachment. Location of the geological map and cross-section presented in Figure  
1654 3 is shown.

1655

1656 **Figure 3.** Geological map and cross-section of the Sierra Albarrana Group (based on  
1657 Insúa et al., 1990 and own data), showing location for samples ALBA-01 to ALBA-31.

1658

1659 **Figure 4.** Petrographic microphotographs showing textural features of the most  
1660 representative rocks in the Sierra Albarrana Group. (A) Fine-grained feldspathic  
1661 metaquartzite from Albarrana Succession; (B) Paragneiss from Cabril-Peña Grajera  
1662 Succession; (C) Fine-grained metagreywacke from Cabril-Peña Grajera Succession (D)  
1663 Fine-grained micaschist from Albariza-Bembézar Succession; (E) Fine-grained garnet  
1664 bearing phyllite from Albariza-Bembézar Succession; (F) Fine-grained metagreywacke  
1665 from Albariza-Bembézar Succession; (G) Fine-grained phyllite from Azuaga Formation;  
1666 and (H) Metagreywacke from Azuaga Formation.

1667

1668 **Figure 5.** (A) Chemical classification diagram for siliciclastic sediments (Herron, 1988).  
1669 (B)  $K_2O$  vs. Chemical Index of Alteration (CIA; after Nesbitt and Young, 1982) for  
1670 comparison of the source area weathering and recycling in Sierra Albarrana  
1671 metasedimentary rocks. Post Archean Australian Shale (PAAS; Taylor and McLennan,  
1672 1985) has been included for comparison.

1673

1674 **Figure 6.** Chondrite normalized rare earth element plots: (A) Metasedimentary rocks  
1675 from Albarrana (AS) and Cabril-Peña Grajera (CGS) successions (Samples ALBA-01 to  
1676 ALBA-11); (B) Metasedimentary rocks from Albariza-Bembézar Succession (ABS) and  
1677 Azuaga Formation (AzF) (Samples ALBA-12 to ALBA-31). Normalizing values are  
1678 from Nakamura (1974). The dotted line corresponds to the PAAS (Post Archean  
1679 Australian Shale; Taylor and McLennan, 1985). (C) PAAS-normalized trace elements

1680 multi-variation diagrams of the Early Cambrian quartzites from Albarrana Succession  
1681 (AS - Sierra Albarrana Group).

1682

1683 **Figure 7.** Provenance discrimination diagrams. (A) Cr/V vs. Y/Ni diagram. The curved  
1684 line represents the model mixing between ultramafic and granitic end-members (after  
1685 Hiscott, 1984; McLennan et al., 1993). (B) Cr/V vs. Sc/Th showing the affinity of the  
1686 metasedimentary rocks from Sierra Albarrana Group for a felsic source.

1687

1688 **Figure 8.** (A) Co/Th vs. La/Sc diagram for provenance discrimination of siliciclastic  
1689 rocks (average compositions of igneous rocks from Condie, 1993). (B) Zr/Ti vs. Nb/Y  
1690 diagram (fields after Winchester and Floyd 1977; Fralick and Kronberg, 2003) showing  
1691 affinity for felsic volcanic rhyolitic/dacitic sources.

1692

1693 **Figure 9.** PAAS-normalized trace elements multi-variation diagrams of the Early  
1694 Cambrian metasedimentary series of the Sierra Albarrana Group (SW Iberian  
1695 Autochthonous Domain). (A) Metasedimentary rocks from Cabril-Peña Grajera  
1696 Succession (CGS); (B) Metasedimentary rocks from Albariza-Bembézar Succession  
1697 (ABS); (C) Metasedimentary rocks from Azuaga Formation (AzF). PAAS after Taylor  
1698 and McLennan (1985). Passive margin shales (after Winchester and Max, 1989), Early  
1699 Cambrian shales from Central Iberian Zone (Fuenlabrada et al., 2016), and Middle  
1700 Cambrian metapelitic rocks from NW Basal Allochthonous Units (Fuenlabrada et al.,  
1701 2012) fields have been included for comparison (see the text for a further explanation).

1702

1703 **Figure 10.** (A) La/Th vs. Hf diagram for active/passive margin source discrimination of  
1704 sandstones (fields from Floyd and Leveridge, 1987; and references therein). (B) Th/Sc

1705 vs. Zr/Sc diagram (after McLennan et al. 1993). Samples plot away from igneous  
1706 compositional variations, suggestive of an increase in sedimentary sorting and recycling.

1707

1708 **Figure 11.** TDM model ages (after DePaolo, 1981) of the Early Cambrian  
1709 metasedimentary series from the Sierra Albarrana Group (SW Iberian Autochthonous  
1710 Domain). TDM model ages of Early Cambrian metasedimentary sequences from Central  
1711 Iberian Zone (Fuenlabrada et al., 2016), and TDM model ages of Sierra Albarrana Group  
1712 (López-Guijarro et al., 2008) have been included for comparison.

1713

1714 **Figure 12.** (A) Simplified model (not to scale) of an Early Cambrian retro-arc basin for  
1715 the SW Iberian Autochthonous Domain (Sierra Albarrana Group). (B) Schematic  
1716 paleogeographic reconstruction model (not to scale) for the Gondwanan margin during  
1717 the approximate Ediacaran-Cambrian transition (c. 540 Ma) (after Albert et al., 2015;  
1718 Brahimí et al., 2018). Iberian sedimentary basins locations are shown in relation to the  
1719 main North African cratonic masses. CIZ - Central Iberian Zone. OMC (Ossa-Morena  
1720 Complex), AM (Armorican Massif), and SXTZ (Saxo-Thuringian Zone) locations  
1721 according to Rojo-Pérez et al., submitted. Arrows show the probable provenance for the  
1722 detrital materials (*see text for further explanation*).

1723

1724

Figure 1

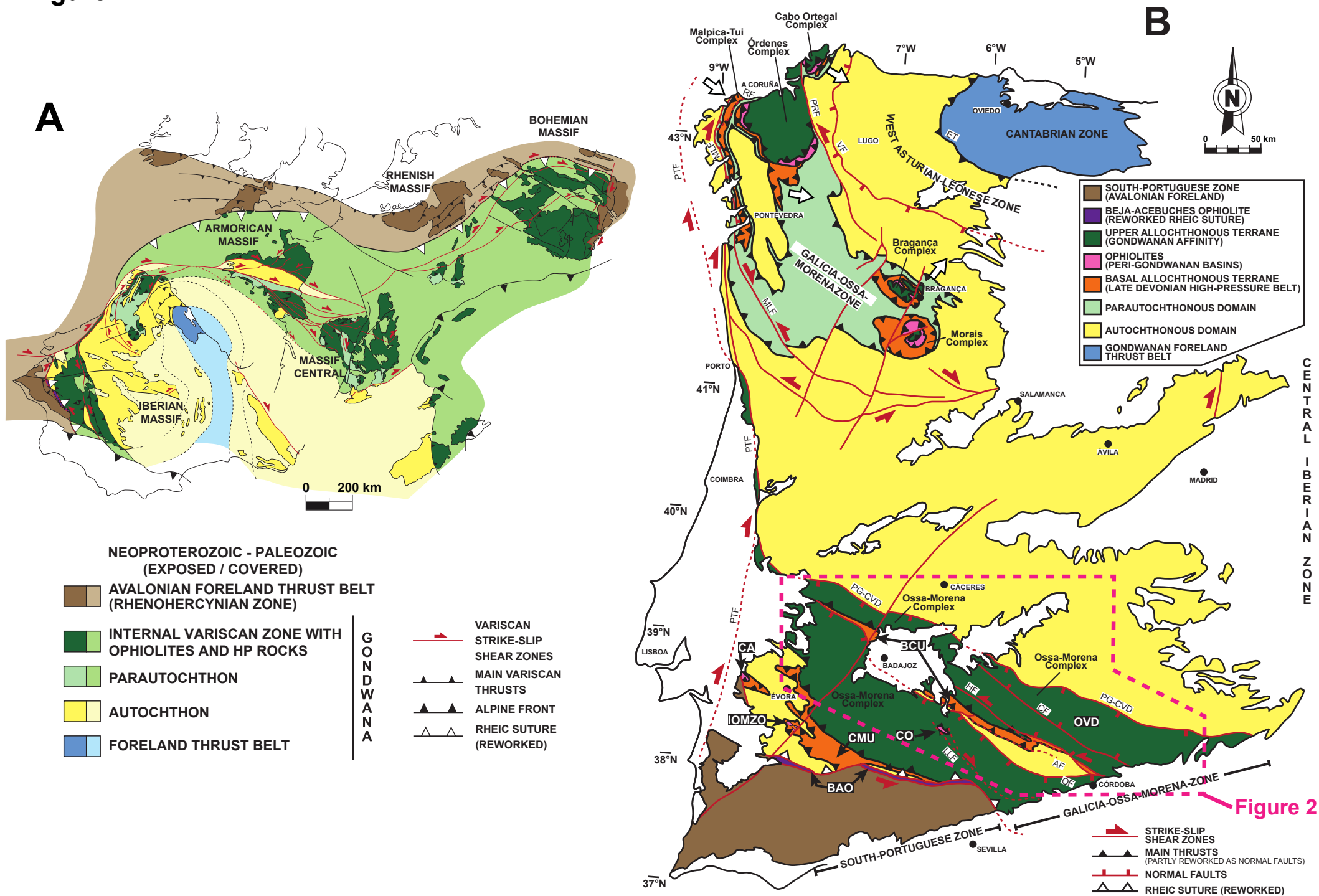


# Figure 2

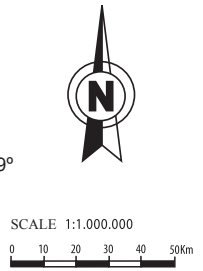
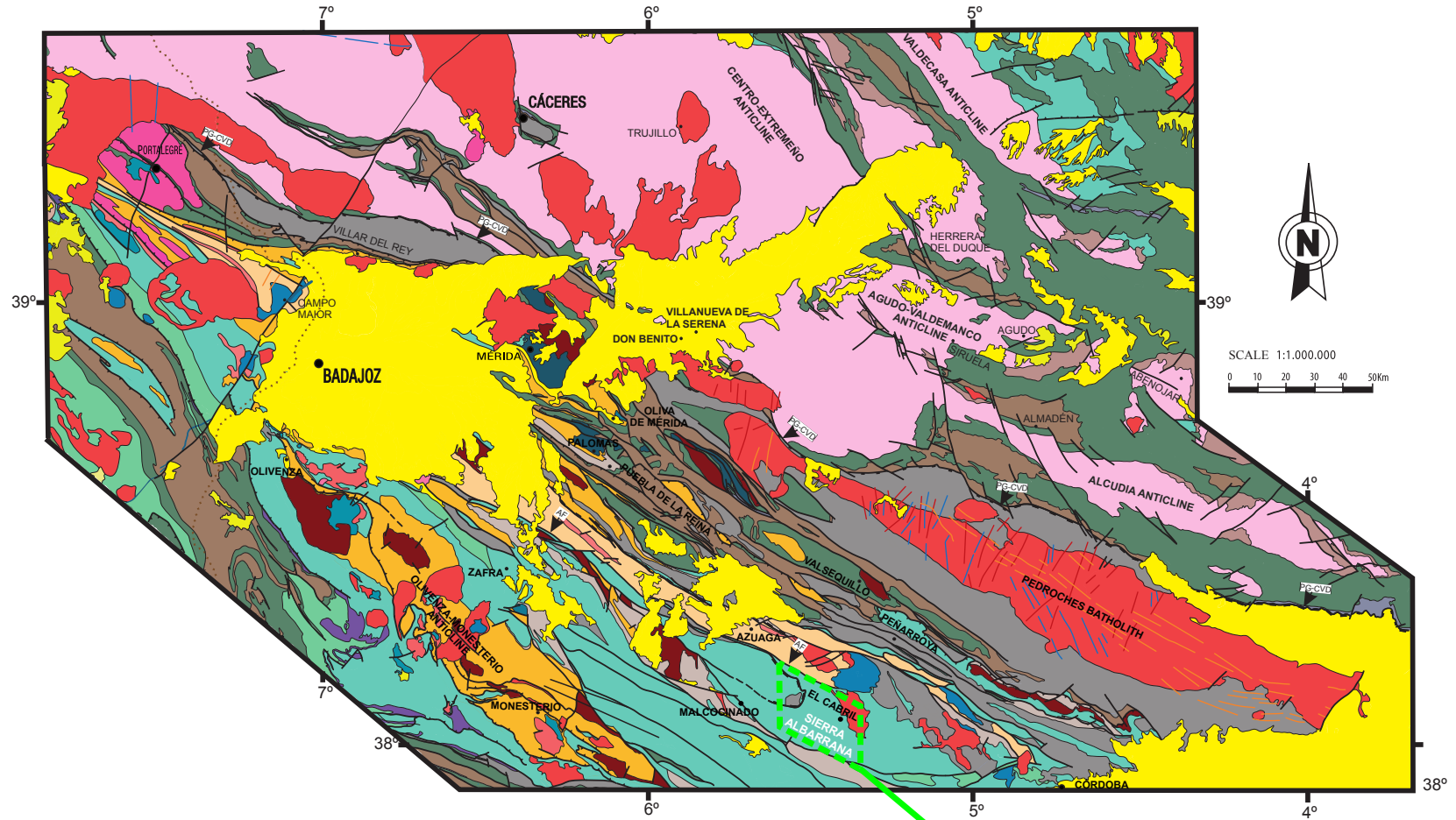


Figure 3

- |   |   |  |
|---|---|--|
| <p><b>EDIACARAN</b></p> <ul style="list-style-type: none"> <li>MALCOGINADO FM: SHALES, VOLCANIC ROCKS AND MIGMATITES</li> <li>UPPER ALCUDIAN FM: SCHISTS, GREYWAKES AND CARBONATE LEVELS</li> <li>LOWER ALCUDIAN FM: SCHIST-GREYWAKE COMPLEX FM: SCHISTS, GREYWAKES QUARTZITES AND CONGLOMERATES</li> <li>SERIE NEGRAFM: SCHISTS, GREYWAKES, SHALES AND BLACK QUARTZITES</li> </ul> <p><b>CAMBRIAN</b></p> <ul style="list-style-type: none"> <li>METASEDIMENTARY AND METAVOLCANIC ROCKS</li> <li>BASALTS</li> <li>SCHISTS, METASANDSTONES, MARBLES, CONGLOMERATES AND METAVOLCANIC ROCKS</li> </ul> <p><b>DEVONIAN - SILURIAN</b></p> <p><b>ORDOVICIAN</b></p> <p><b>CARBONIFEROUS</b></p> <p><b>CENOZOIC AND QUATERNARY</b></p> | <p><b>EDIACARAN PLUTONISM</b></p> <ul style="list-style-type: none"> <li>FELSIC AND INTERMEDIATE ROCKS</li> <li>MAFIC AND ULTRAMAFIC ROCKS</li> </ul> <p><b>CAMBRO-ORDOVICIAN PLUTONISM</b></p> <ul style="list-style-type: none"> <li>ALKALINE GRANITOIDS</li> <li>MAFIC AND ULTRAMAFIC ROCKS</li> <li>CALC-ALKALINE AND PERALUMINIC GRANITOIDS AND/OR AUGEN ORTHOGNEISSES</li> </ul> <p><b>VARISCAN PLUTONISM</b></p> <ul style="list-style-type: none"> <li>GRANITOIDS</li> <li>MAFIC AND ULTRAMAFIC ROCKS</li> <li>DIKES AND OTHER SIMILAR BODIES</li> </ul> <p><b>CENTRAL UNIT</b></p> <ul style="list-style-type: none"> <li>BLASTOMYLONITIC GNEISSES, MIGMATITES, AMPHIBOLITES, ECLOGITES</li> </ul> | <ul style="list-style-type: none"> <li>— FAULT</li> <li>— DETACHMENT</li> <li>— CONTACT</li> <li>— THRUST</li> <li>AF: AZUAGA FAULT</li> <li>PG-CVD: PUENTE GÉNAVE-CASTELO DE VIDE DETACHMENT</li> </ul> |
|---|---|--|



**SYN-OROGENIC SERIES**

**CARBONIFEROUS**

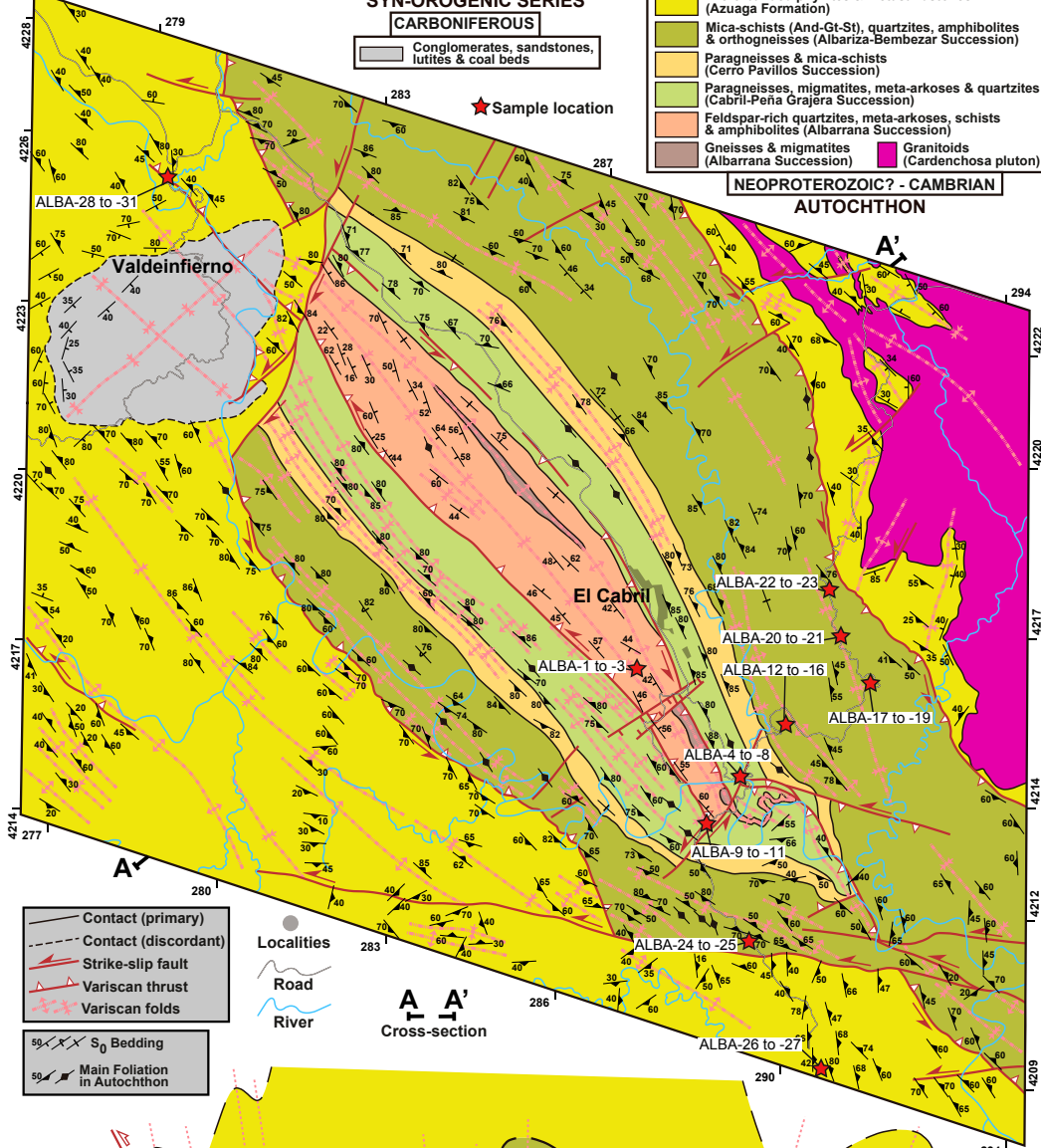
Conglomerates, sandstones, lutites & coal beds

★ Sample location

- Micro-banded phyllites & metasandstones (Azuaga Formation)
- Mica-schists (And-Gt-St), quartzites, amphibolites & orthogneisses (Albariza-Bembezar Succession)
- Paragneisses & mica-schists (Cerro Pavillos Succession)
- Paragneisses, migmatites, meta-arkoses & quartzites (Cabril-Peña Grajera Succession)
- Feldspar-rich quartzites, meta-arkoses, schists & amphibolites (Albarana Succession)
- Gneisses & migmatites (Albarana Succession)
- Granitoids (Cardenchosa pluton)

**NEOPROTEROZOIC? - CAMBRIAN**

**AUTOCHTHON**



- Contact (primary)
- Contact (discordant)
- Strike-slip fault
- Variscan thrust
- Variscan folds
- S<sub>0</sub> Bedding
- Main Foliation in Autochthon

Localities

Road

River

A A'  
Cross-section

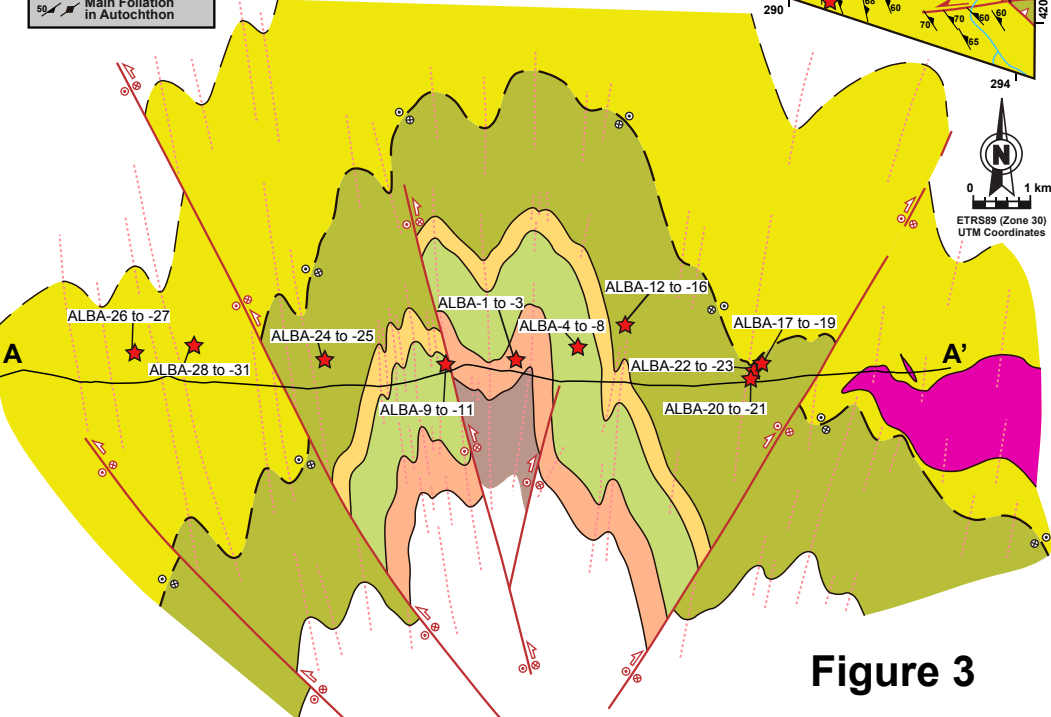


**Figure 3**

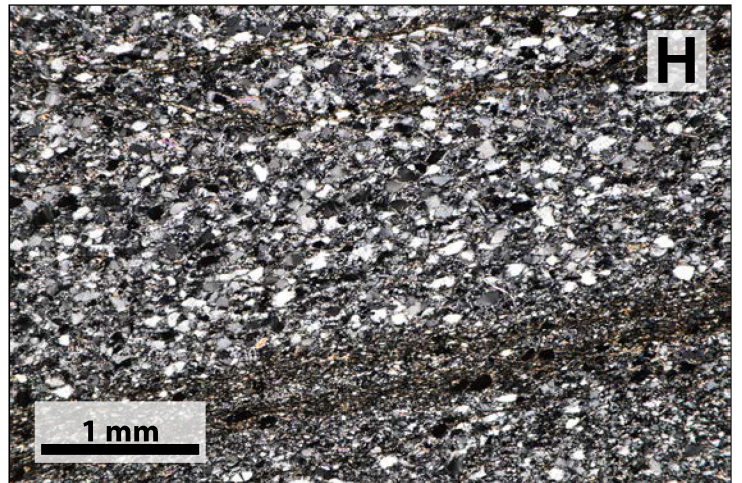
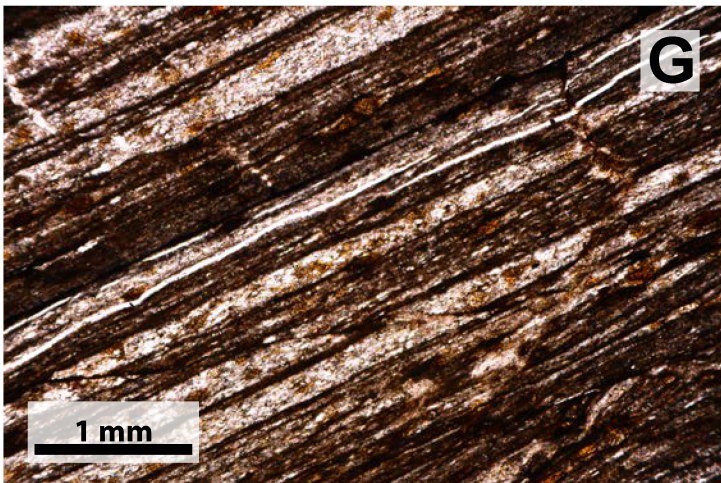
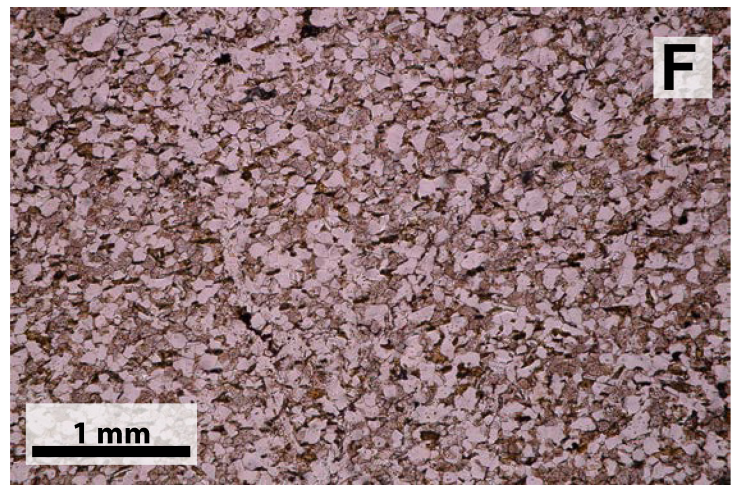
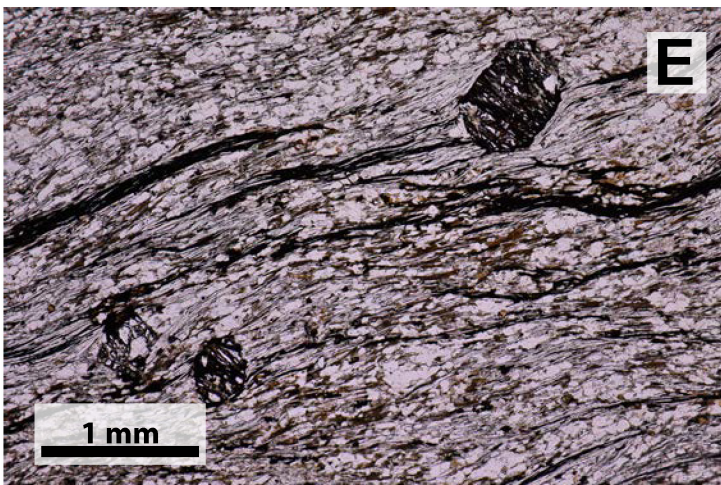
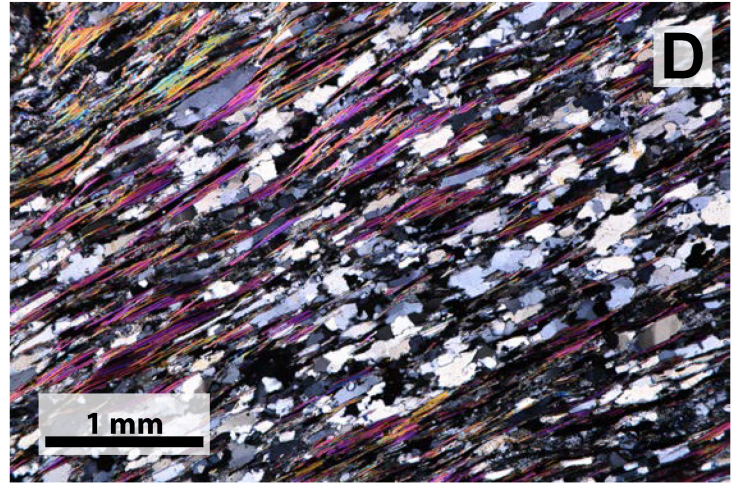
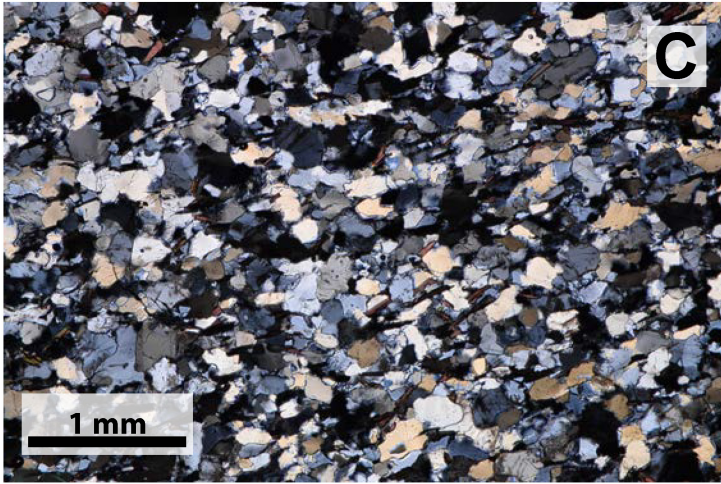
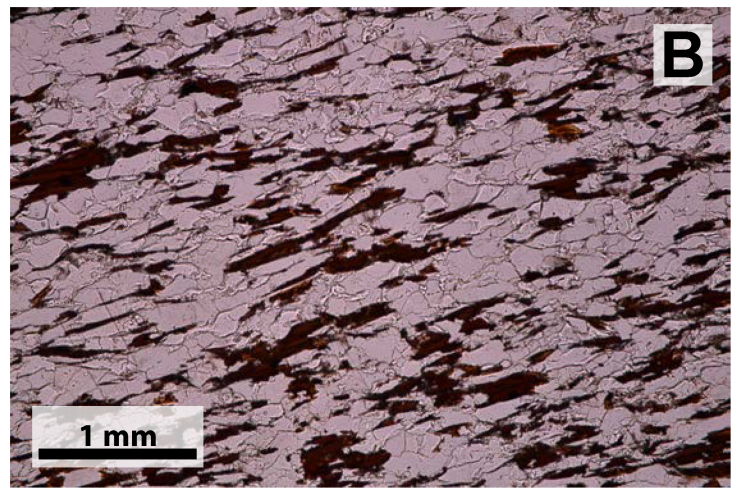
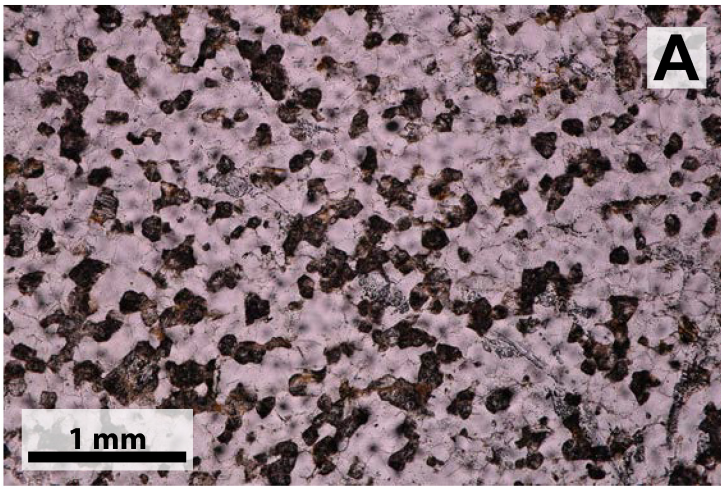
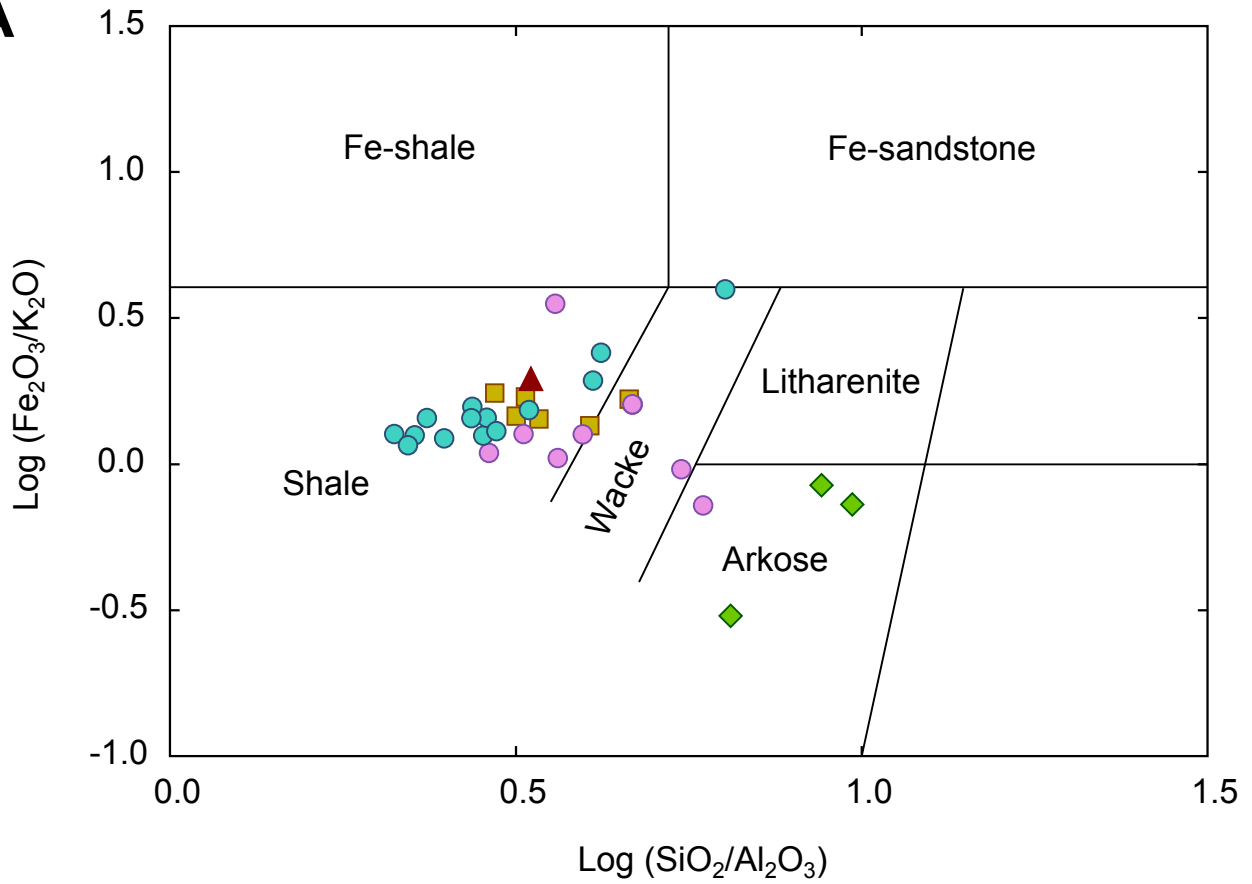
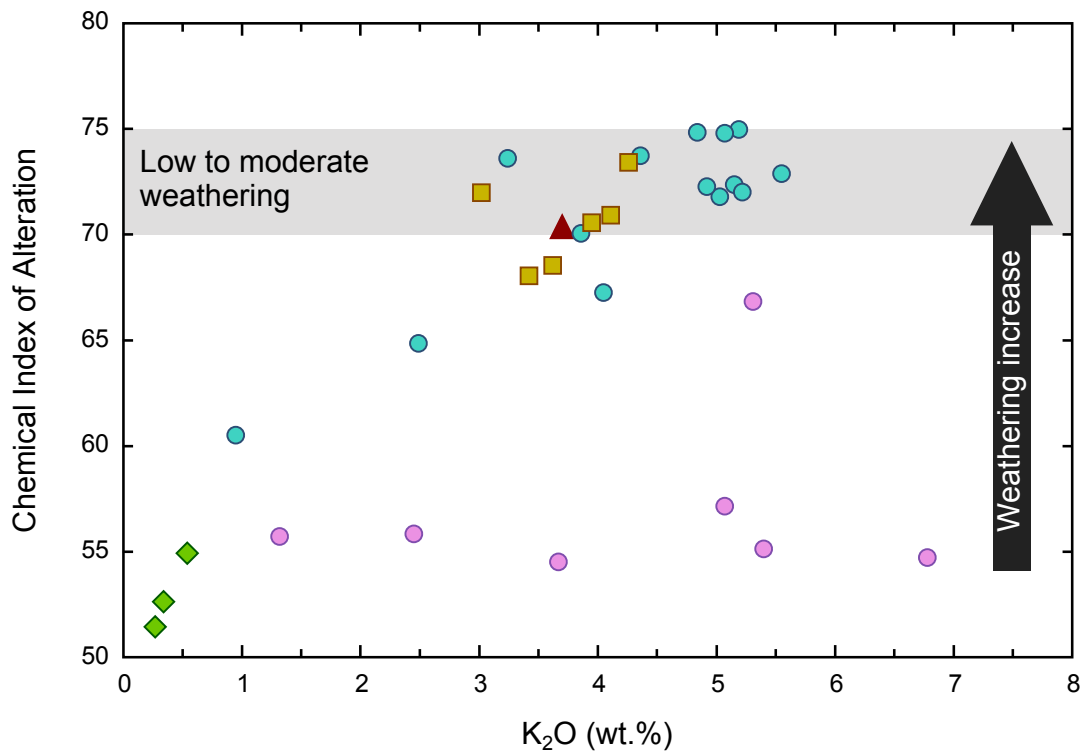


Figure 5

A



B



- ◆ Quartzites (Albarrana Succession - AS)
- Metasedimentary rocks (Cabril-Peña Grajera Succession - CGS)
- Metasedimentary rocks (Albariza-Bembézar Succession - ABS)
- Metasedimentary rocks (Azuaga Formation - AzF)
- ▲ Post Archean Australian Shale (PAAS)

**Figure 6**

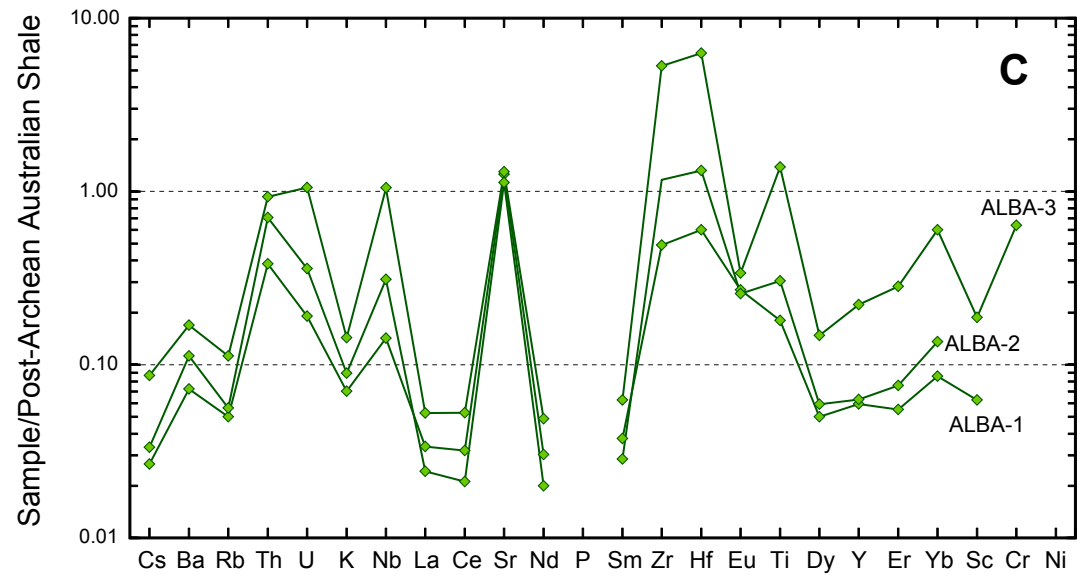
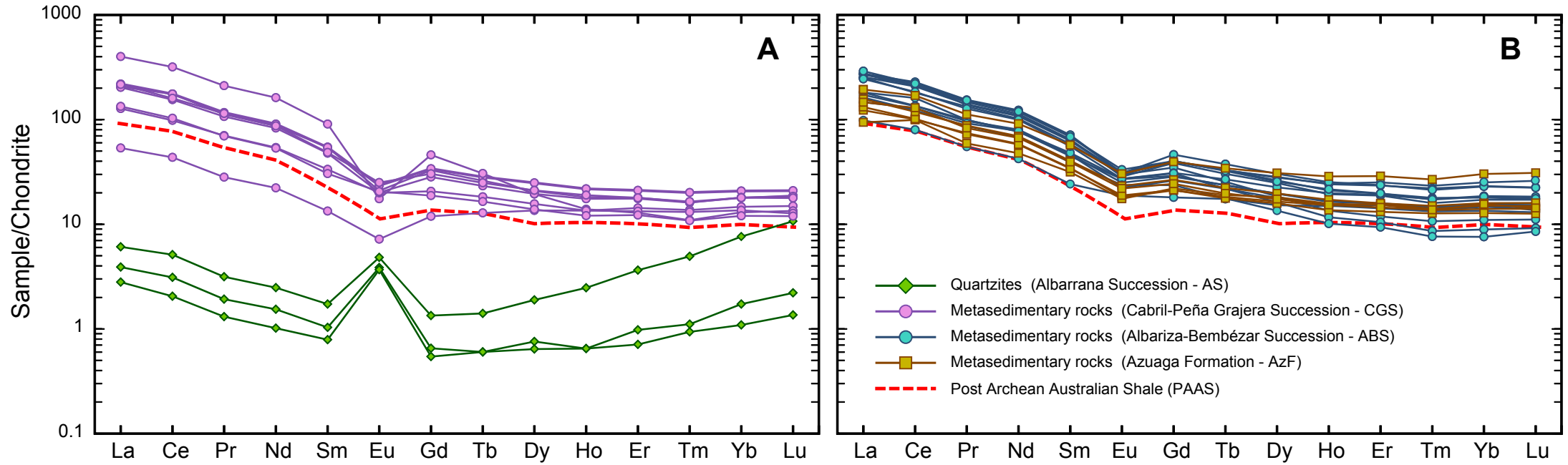
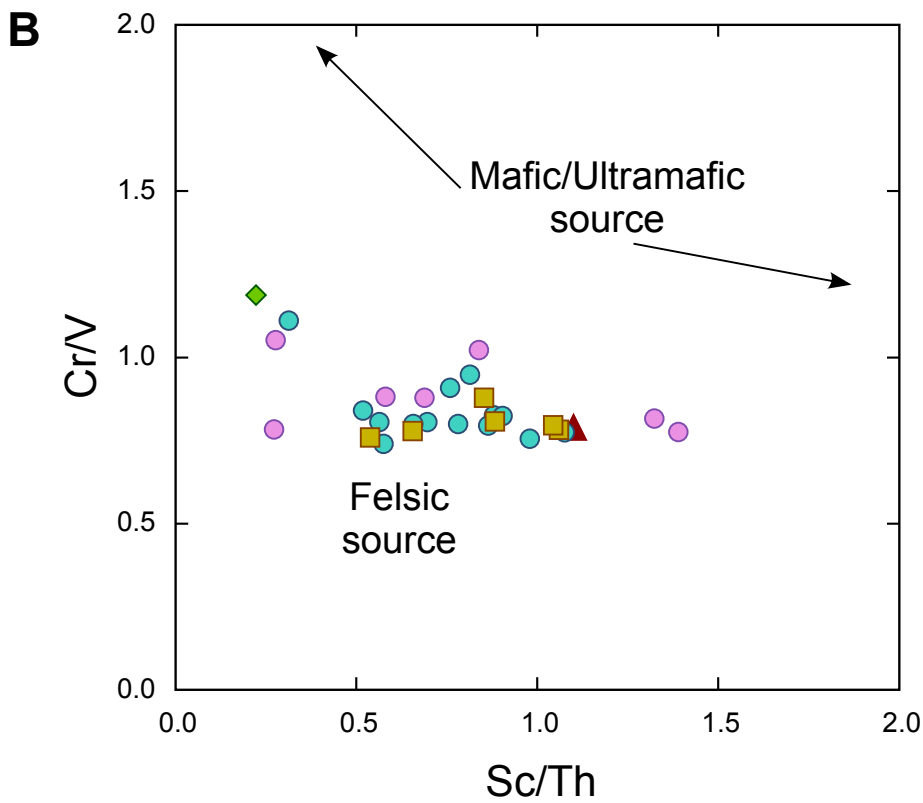
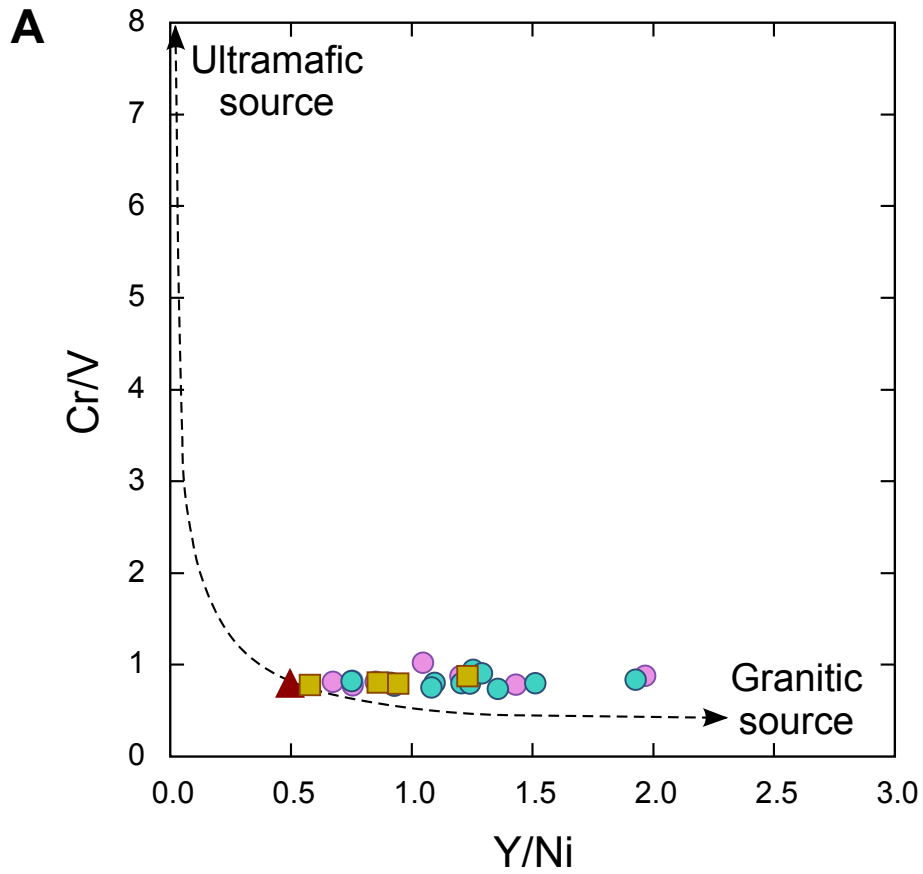
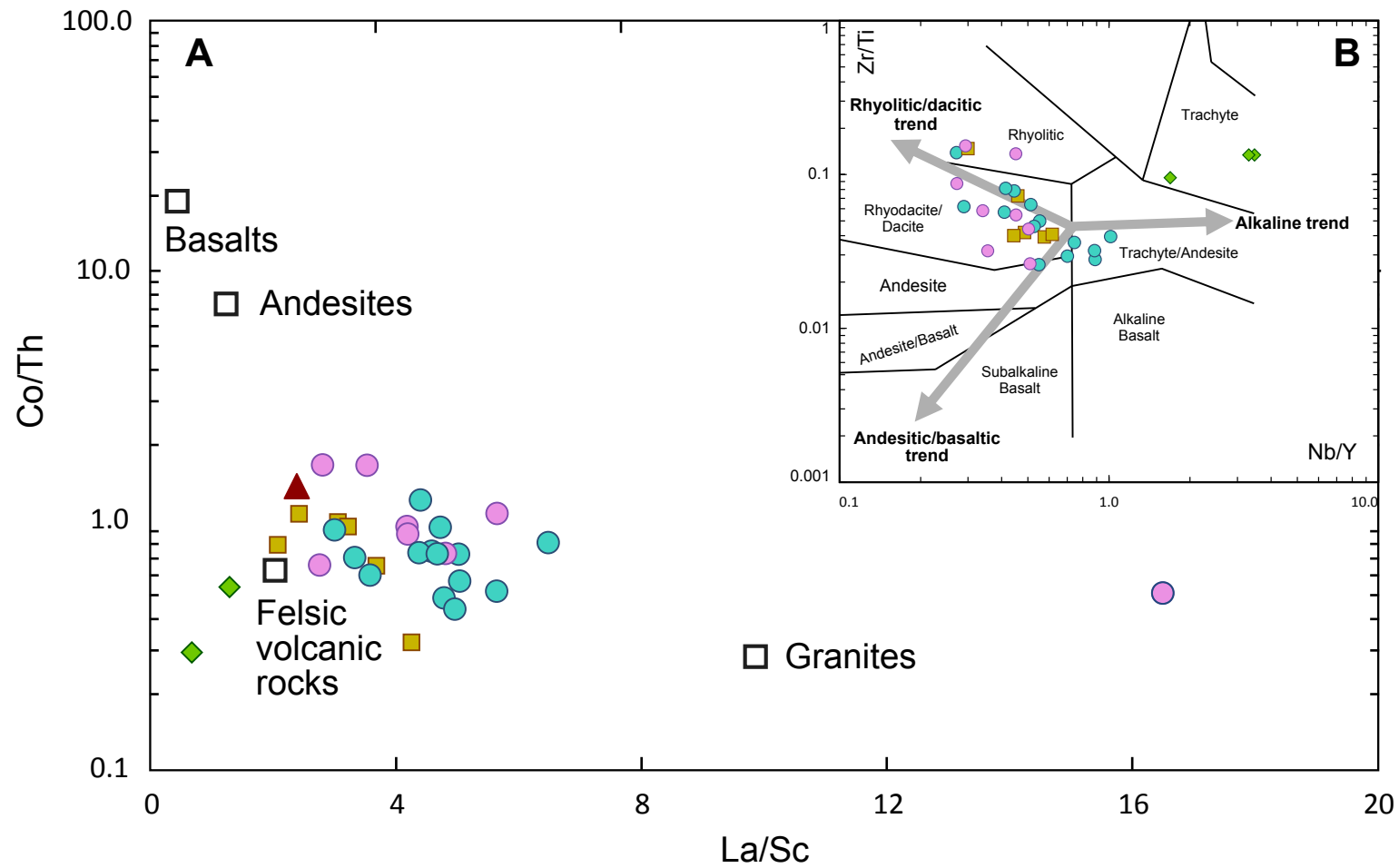


Figure 7



- Metasedimentary rocks (Cabril-Peña Grajera Succession - CGS)
- Metasedimentary rocks (Albariza-Bembézar Succession - ABS)
- Metasedimentary rocks (Azuaga Formation - AzF)
- ◆ Quartzites (Albarrana Succession - AS)
- ▲ Post Archean Australian Shale (PAAS)

**Figure 8**



- ◆ Quartzites (Albarrana Succession - AS)
- Metasedimentary rocks (Cabril-Peña Grajera Succession - CGS)
- Metasedimentary rocks (Albariza-Bembézar Succession - ABS)
- Metasedimentary rocks (Azuaga Formation - AzF)
- ▲ Post Archean Australian Shale (PAAS)

**Figure 9**

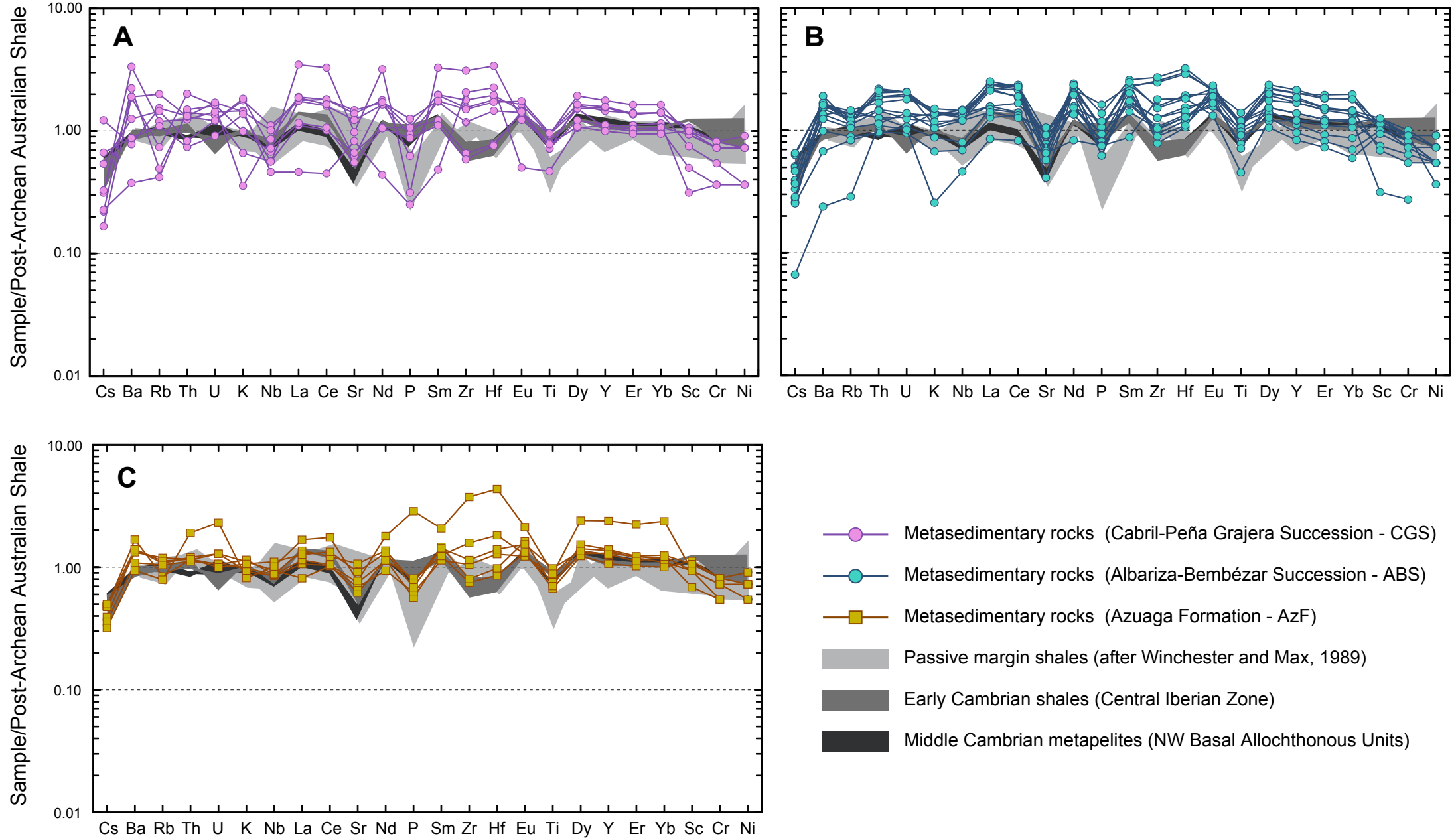
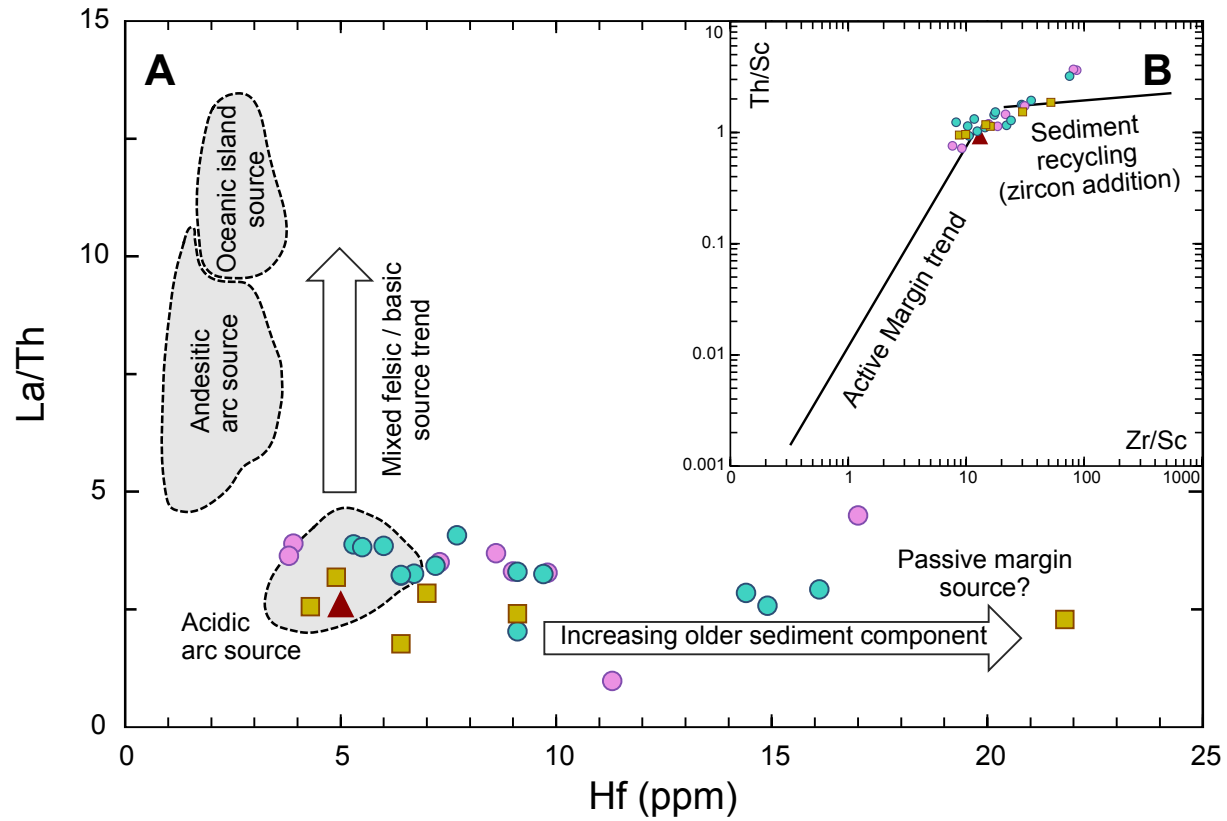


**Figure 10**



- Metasedimentary rocks (Cabril-Peña Grajera Succession - CGS)
- Metasedimentary rocks (Albariza-Bembézar Succession - ABS)
- Metasedimentary rocks (Azuaga Formation - AzF)
- ▲ Post Archean Australian Shale (PAAS)



**Figure 11**

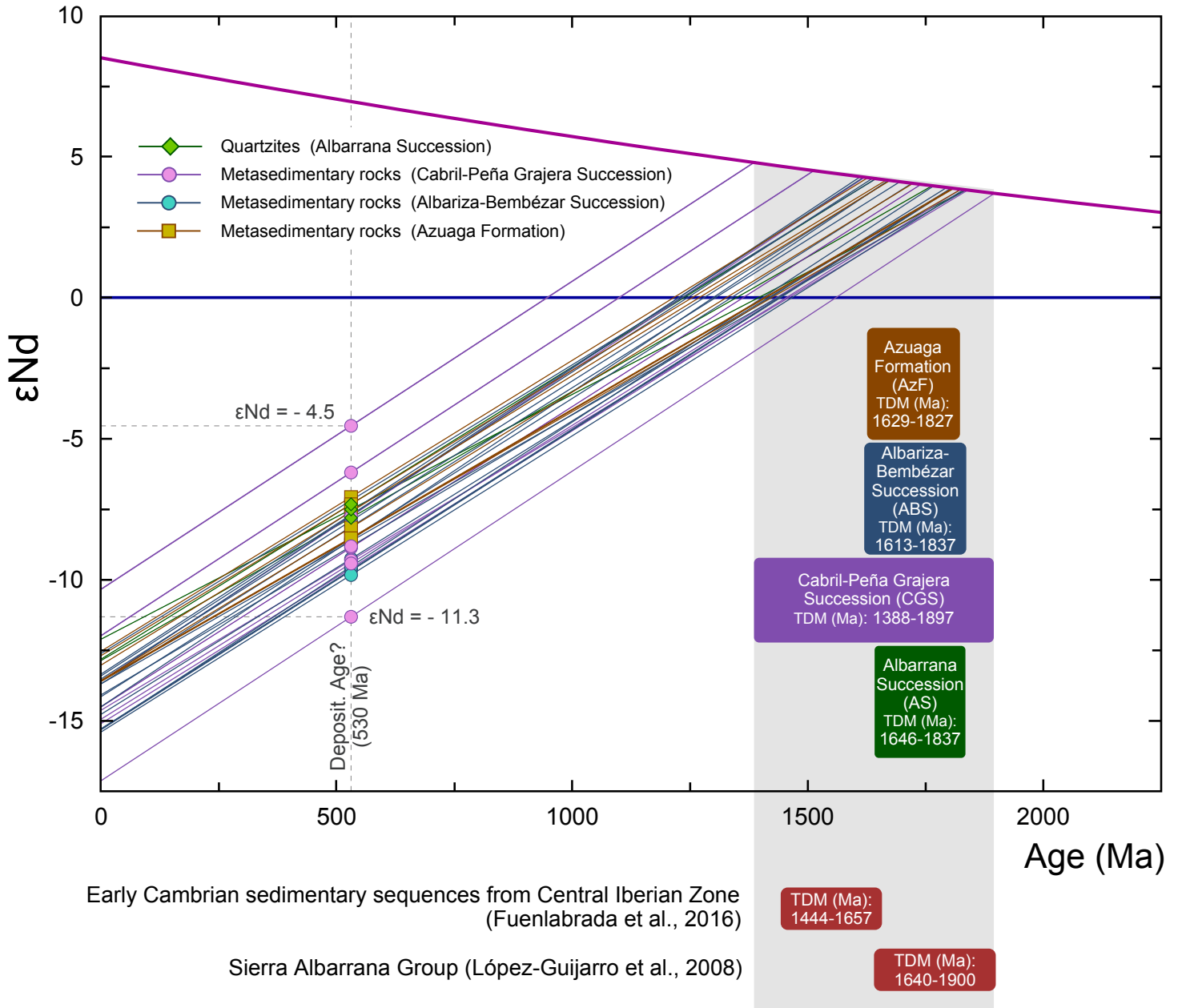
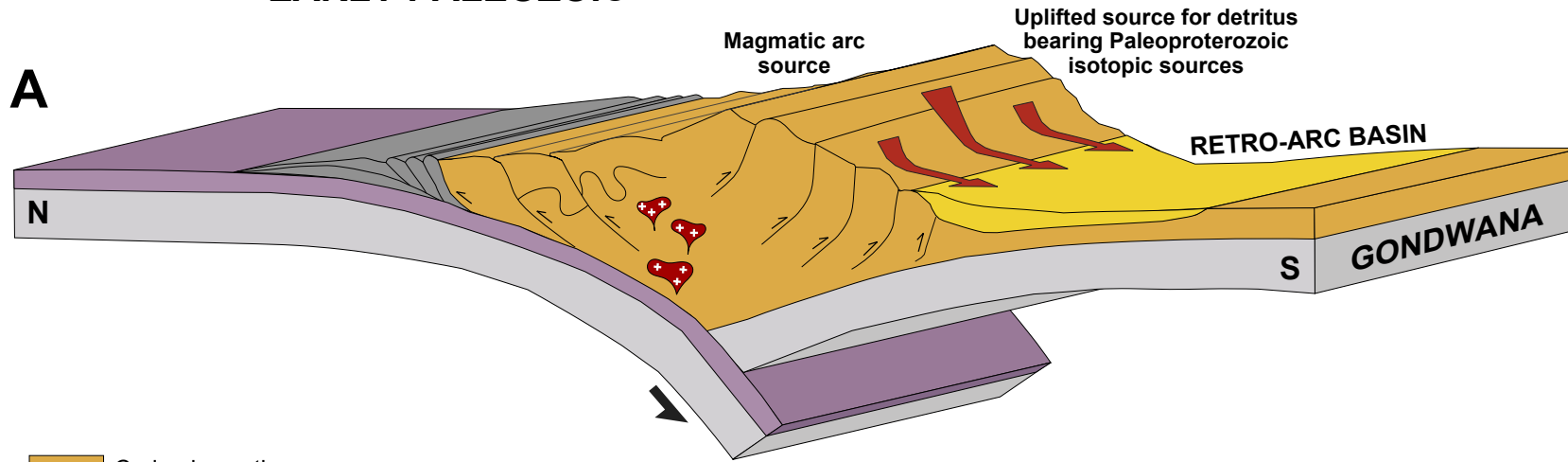


Figure 12

EARLY PALEOZOIC



- Cadomian active arc
- Early Cambrian sedimentary basins (SW Iberia Autochthonous Domain)
- + + + Arc-related plutonic intrusions
- Accretionary wedge
- Oceanic crust
- Mantle Lithosphere
- Sediments flow direction

c. 540 Ma

